HHS Public Access

Author manuscript

J Comp Neurol. Author manuscript; available in PMC 2021 April 29.

Published in final edited form as:

J Comp Neurol. 2017 April 01; 525(5): 1291–1311. doi:10.1002/cne.24137.

In vivo transgenic expression of collybistin in neurons of the rat cerebral cortex

Christopher D. Fekete, **Roman U. Goz**, **Sean Dinallo**, **Celia P. Miralles**, **Tzu-Ting Chiou**, **John Bear Jr.**, **Christopher G. Fiondella**, **Joseph J. LoTurco**, **Angel L. De Blas**

Department of Physiology and Neurobiology, University of Connecticut, Storrs, Connecticut, 06269, USA.

Abstract

Collybistin (CB) is a guanine nucleotide exchange factor selectively localized to GABAergic and glycinergic postsynapses. Active CB interacts with gephyrin inducing the submembranous clustering and the postsynaptic accumulation of gephyrin, which is a scaffold protein that recruits $GABA_A$Rs at the postsynapse. CB is expressed with or without a *src homology 3* (SH3) domain. We have previously reported the effects on GABAergic synapses of the acute overexpression of $CB_{\mathbf{SH3}-}$ or $CB_{\mathbf{SH3}+}$ in cultured hippocampal (HP) neurons. In the present communication, we are studying the effects on GABAergic synapses after chronic *in vivo* transgenic expression of $CB2_{\mathbf{SH3}-}$ or $CB2_{\mathbf{SH3}+}$ in neurons of the adult rat cerebral cortex. The embryonic precursors of these cortical neurons were *in utero* electroporated with $CB_{\mathbf{SH3}-}$ or $CB_{\mathbf{SH3}+}$ DNAs, migrated to the appropriate cortical layer, and became integrated in cortical circuits. The results show that i) the strength of inhibitory synapses *in vivo* can be enhanced by increasing the expression of CB in neurons and ii) there are significant differences in the results between *in vivo* and in culture studies.

Keywords

In utero electroporation; collybistin; gephyrin; vesicular GABA transporter; synapse formation; $GABA_A$ receptors; GABAergic synapse; GABAergic synaptic plasticity; GABAergic synaptic strength; RGD_2312511; AB_887873; AB_2232546; AB_10064220; AB_2314482; SCR 014479; SCR_002285; SCR_002815; SCR_013674; SCR_002865

Corresponding author: Angel L. De Blas, PhD, Department of Physiology and Neurobiology, University of Connecticut, 75 N. Eagleville Road, U-3156, Storrs, Connecticut, USA, 06269-3156, Tel.: (860) 486-5440; Fax: (860) 486-5439, angel.deblas@uconn.edu.

ROLES OF AUTHORS

Study concept and design: A.L.D. and J.J.L. Experimental design and acquisition of data: C.D.F., R.G., S.D., C.P.M., T-T.C, J.B.Jr. and C.G.F. Analysis and interpretation of data: C.D.F., R.G. S.D., C.P.M., T-T.C, J.J.L. and A.L.D. Drafting of the manuscript: A.L.D., C.D.F. and R.G. Critical revision of the manuscript for important intellectual content: C.D.F., R.G. C.P.M., J.J.L. and A.L.D. Statistical analysis: C.F., R.G. and A.L.D. Obtained funding: A.L.D. and J.J.L. Study supervision: C.P.M., J.J.L and A.L.D.

CONFLICT OF INTEREST

The authors declare that they have no conflicts of interest with the contents of this article. The content is solely the responsibility of the authors and does not necessarily represent the official views of the National Institutes of Health.

INTRODUCTION

Collybistin (CB) is a guanine nucleotide exchange factor (GEF) selectively localized at GABAergic and glycinergic postsynapses (Chiou et al., 2011; Patrizi et al., 2012). CB interacts with Gephyrin (Geph), a scaffold protein that selectively forms postsynaptic lattices at GABAergic and glycinergic postsynapses (Grosskreutz et al., 2001; Tretter et al., 2012; Tyagarajan and Fritschy, 2014). In host HEK293 or COS-7 cells, active CB induces the submembranous clustering of Geph (Harvey et al., 2004; Kins et al., 2000; Rees et al., 2003). CB-deficient mice show a significant and large decrease in postsynaptic $GABA_A$Rs and Geph clusters in various brain regions including hippocampus, amygdala, cerebellum and some regions of the thalamus among other brain areas (Luscher et al., 2011; Papadopoulos et al., 2008; Papadopoulos et al., 2007; Tyagarajan and Fritschy, 2014; Tyagarajan et al., 2011). Mutations in the human X-linked CB ortholog, hPEM2 (ARHGEF9), have been identified as the cause of hyperekplexia, severe mental retardation and epilepsy (Harvey et al., 2004; Harvey et al., 2008; Kalscheuer et al., 2009; Lemke et al., 2012; Lesca et al., 2011; Machado et al., 2015; Marco et al., 2008; Shimojima et al., 2011).

CB has three major functional domains: i) a *src homology 3* (SH3); ii) a *guanine nucleotide exchange factor* (Rho GEF) that selectively catalyzes GDP-GTP exchange on the small GTPase Cdc42 (Kins et al., 2000; Reid et al., 1999) and iii) a *pleckstrin-homology* (PH) domain (Fritschy et al., 2012). Rodents express three isoforms of CB (CB1, CB2 and CB3) that are splice variants of the same gene and differ in the C-terminus (Harvey et al., 2004). Only CB2 and CB3 are expressed in adult rodent neurons. There are also splice variants of CB2 ($CB2_{\mathbf{SH3}+}$ and $CB2_{\mathbf{SH3}-}$) and CB3 ($CB3_{\mathbf{SH3}+}$ and $CB3_{\mathbf{SH3}-}$) with or without the SH3 domain (Harvey et al., 2004; Kins et al., 2000). The human CB (hPEM2) is equivalent to rodent CB3 and also has SH3+ and SH3− variants (Kins et al., 2000).

We have reported that CB is a rate-limiting regulator of postsynaptic $GABA_A$R and Geph clustering in cultured HP neurons (Chiou et al., 2011). Overexpression of $GABA_A$Rs or Geph does not significantly affect synaptic $GABA_A$R/Geph clustering (Chiou et al., 2011). In contrast, overexpression of $CB2_{\mathbf{SH3}-}$ in cultured HP neurons induces the formation of very large Geph and $GABA_A$R synaptic clusters (superclusters), whereas $CB2_{\mathbf{SH3}+}$ leads to higher (supernumerary) number of smaller and frequently non-synaptic Geph and $GABA_A$R clusters (Chiou et al., 2011). Similar effects on Geph clustering were reported by other laboratories studying acute overexpression of CB in neuronal cultures (Kalscheuer et al., 2009; Papadopoulos et al., 2015; Soykan et al., 2014; Tyagarajan et al., 2011). In the present communication, we have investigated the effects on GABAergic synapses after long-term *in vivo* CB overexpression in cerebral cortex neurons that are developmentally and functionally integrated in brain circuits.

MATERIALS AND METHODS

Animals

Pregnant Wistar rats were obtained from Charles River Laboratories, Inc. (Wilmington, MA; RRID: RGD_2312511). Both male and female embryos were used in the experiments. The

animal protocols were approved by the Institutional Animal Care and Use Committee and followed the National Institutes of Health guidelines.

Antibodies

Table 1 summarizes the primary antibodies used in this study.

The guinea pig (GP) anti-vGAT antibody (catalog# 131004; lot# 131004/13; RRID:AB_887873; dilution 1:1,000) was purchased from Synaptic Systems (Gottingen, Germany). In cultured hippocampal neurons and brain sections this antibody shows puncta staining apposed to Geph clusters. The manufacturer's verification of the specificity of this antibody include mouse K.O. verification. The mouse (Ms) monoclonal antibody (mAb) to Geph (clone mAb7a; catalog# 147021; lot# 147021/9; RRID:AB_2232546; dilution 1:200) was from Synaptic Systems. The antibody shows punctate labelling in hippocampal neuron cultures and brain sections that colocalizes highly with antibodies to $GABA_A$ receptor subunits. It also labels a 93kD band and a weaker 48kD band in immunoblots of purified glycine receptor/gephyrin complex from the rat spinal cord (Pfeiffer et al., 1984). This antibody is listed in the JCN database. The Rabbit (Rb) anti-CB antibody (catalog# 261003; lot# 261003/3; dilution 1:500) was from Synaptic Systems. The Ms anti-HA epitope (catalog# MMS-101R; Clone 16B12; lot# E11EF01029; RRID:AB_10064220; dilution 1:500) was from Covance (Princeton, NJ). The Rb anti-CB and the Ms anti-HA antibodies co-label HEK293 cells transfected with HA-$CB2_{SH3-}$ and HA-$CB2_{SH3+}$ constructs in culture and co-labeled the same protein band in immunoblots of the transfected HEK293 cells. The Rb antibody to the γ2 subunit (RRID:AB_2314482) of the rat $GABA_AR$ (to amino acids 1–15 QKSDDDYEDYASNKT) was raised and affinity-purified (on immobilized antigen peptide) in our laboratory (dilution 1:10). In cultured hippocampal neurons this antibody shows clustered labelling that colocalizes highly with that of antibodies to other $GABA_A$ receptor subunits (Gp anti-γ2, Rb anti-α1, Rb anti-α2, and Ms mAb anti-β2/3) and to Geph. It shows apposition to glutamate decarboxylase (GAD)-containing terminals. Immunofluorescence can be blocked with the antigenic peptide. This antibody is in the JCN database and it has been described and characterized elsewhere (Charych et al., 2004a; Charych et al., 2004b; Chiou et al., 2011; Christie and De Blas, 2003; Christie et al., 2002a; Christie et al., 2006; Christie et al., 2002b; Fekete et al., 2015; Jin et al., 2014; Li et al., 2005; Li et al., 2007; Li et al., 2010; Li et al., 2012; Yu and De Blas, 2008; Yu et al., 2007).

For immunofluorescence in tissue sections, species specific anti-IgG secondary antibodies raised in goat were used. These antibodies were labeled with either Alexa Fluor 488, 568, or 647 (Invitrogen, Eugene, OR).

Plasmids

After testing several expression plasmids and protein tags in previous IUEP studies for transgenic overexpression of various tagged proteins, we have adopted the pCAGGS plasmid and the hemagglutinin (HA) tag as the most suitable for obtaining both high protein expression and reliable immunofluorescence localization of the transgenically expressed

protein in adult rat brain slices. Thus we subcloned rat HA-CB2$_{\mathbf{SH3}-}$ and HA-CB2$_{\mathbf{SH3}+}$ in pCAGGS.

The rat cmyc-CB2$_{\mathbf{SH3}-}$ and cmyc-CB2$_{\mathbf{SH3}+}$ (both in pRK5) were provided by Drs. Kirsten Harvey and Robert Harvey (University College of London School of Pharmacy, UK).

In utero electroporation (IUEP)

In utero electroporation was performed as previously described (Bai et al., 2003; Chen and LoTurco, 2012; Li et al., 2005; Li et al., 2010; Ramos et al., 2006). Briefly, pregnant rats were anesthetized with a mixture of ketamine-HCl/xylazine (100/10 mg/kg) or a mixture of ketamine-HCl/xylazine/acepromazine maleate (60/8/2 mg/kg) and laparotomy was performed. Metacam analgesic was administered daily at dosage of 1 mg/kg for 2 days following surgery. To visualize the plasmid suspension during injection in the lateral ventricle, plasmids were mixed with 2 mg/ml Fast Green (Sigma, St Louis, MO). In all conditions, pCAG-EGFP, pCAGGS-HA-CB2$_{\mathbf{SH3}+}$, pCAGGS-HA-CB2$_{SH3-}$, were used at the final concentration of 1.5 μg/μl. To target layer 2/3 of somatosensory cortex, electroporation was performed at embryonic day 14 or 15 (E14 or E15). During surgery, the uterine horns were exposed and one lateral ventricle of each embryo was pressure injected with 1–2 μl of plasmid DNA. Microinjections were made through the uterine wall and embryonic membranes by inserting a pulled glass microelectrode (Drummond Scientific, Broomall, PA) into the lateral ventricle followed by pressure injection with pulses delivered with a Picospritzer II (General Valve, Fairfield, NJ). Electroporation was accomplished with a BTX 8300 pulse generator (BTX Harvard Apparatus, Holliston, MA) and BTX tweezertrodes applied to the embryo's head. Electroporation was carried out by a brief (1–2 msec) discharge of a 500-μF capacitor charged to 65–75 V. After electroporation, the uterus was returned to the abdominal cavity, and the incision was closed by sewing it up with sterile surgical suture. With this protocol, and in the region of maximal transfection, others have shown that about 20% of the neurons in layer2/3 of the targeted cortical area are transfected (Rice et al., 2010). Our results are consistent with these observations.

Immunofluorescence of sections from fixative-perfused brains

IUEP embryos were normally born and raised by their mothers. As adults (in all cases at P41-P45, they were deeply anesthetized with a mixture of ketamine HCl/xylazine/ acepromazine maleate (60/8/2 mg/kg) and perfused through the ascending aorta with PB (27 mM NaH2PO4, 92 mM Na2HHPO4, pH 7.4) followed by 4% PLP fixative (4% paraformaldehyde, 1.37% lysine, 0.21% sodium periodate in 0.1 M phosphate buffer, pH 7.4). Brains were cryoprotected with sucrose (30%), frozen, and sectioned with a freezing microtome (25 μm-thick) and stored in 0.02 % NaN_3 in 0.1M Phosphate Buffer (PB) pH7.4 at 4°C. Immunofluorescence was done as described elsewhere (Fekete et al., 2015; Li et al., 2009; Li et al., 2010). Briefly, free-floating brain sections were incubated with 5% normal goat serum (NGS)/0.1 M PB or 5%NGS/0.3% Triton X-100 in 0.1M PB for 1 hour at RT. Sections were then incubated for 2 days in mixtures of primary antibodies raised in different species in 2% NGS/0.3% Triton X-100 in 0.1M PB at 4°C. Sections were washed and incubated in a mixture of fluorophore conjugated secondary antibodies in 2% NGS/ 0.3%Triton in 0.1M PB for 1 hour at RT. Sections were then washed again and mounted

onto gelatin coated glass slides with Prolong Gold Antifade mounting solution and imaged with a laser scanning confocal microscope. With this perfusion-fixation procedure we observe good labeling of GABAergic pre and postsynaptic proteins comparable to that seen using brief post-fixation after cryostat sectioning of rat brain tissue (Schneider Gasser et al., 2006).

Image acquisition, data analysis, and quantification

Confocal images of brain sections were acquired using either a SP2 laser scanning confocal microscope (Leica, Wetzlar, Germany) with a HCX PL Apo 40x/1.25 oil objective or an A1R laser scanning confocal microscope (Nikon Instruments, Tokyo, Japan) with either a Plan Apo VC 60x/1.4 oil objective or a Plan Fluor 40x/1.3 oil objective. The pinhole was set at 1–1.2 Airy units. Images were either collected as single optical sections or in z-stacks taken at 0.5μm steps. Low magnification images of brain sections for EGFP fluorescence in Fig 1A–C were collected by epifluorescence with a Plan Fluor 10x/0.3 objective. For qualitative analysis, images were processed and merged for color colocalization in Photoshop CS5 (Adobe, San Jose, CA).

For quantification of Geph mean fluorescence intensity (MFI), maximal projections of 5 consecutive images from the same z-stack were made using FIJI software (Schindelin et al., 2012) (RRID: SCR_002285). A selection area was then manually drawn around each cell using vGAT or Geph puncta as a guide. A second selection area was then generated 10 pixels inside the first creating a selection band encompassing the outer edge of the cell body. The mean gray value of this band was then calculated for the transfected and non-transfected cells in each image using FIJI software. The same procedure was performed for vGAT but on single optical sections.

To quantify the number and size of Geph and vGAT clusters FIJI was used to subtract the background fluorescence and 15 pixel wide selection areas were drawn around transfected and non-transfected cells, similar to the quantification for MFI. The trainable Weka Segmentation plugin for FIJI software was used to segment the images. The segmented images were converted into binary images and the analyze particle tool was used to calculate the number and size of clusters falling within the individual selection areas. The binary images were also overlaid on the raw image files to manually confirm that the segmentation was adequate. The final quantification graphs were generated with Inkscape (RRID: SCR_014479).

Statistical Analysis

Statistical analysis of the values calculated by FIJI software was performed with InStat 3 (GraphPad, San Diego, CA). For analysis of all immunofluorescence data the non-parametric Mann-Whitney test was used to compare transfected and control non-transfected neurons from the same image sets. For statistical analysis of electrophysiology data SPSS (IBM Corp., Armonk, NY; RRID:SCR_002865) was used. The Kolmogorov-Smirnov test was used to compare the distribution of the measured mIPSC values and Welch ANOVA was used to compare the means with Game-Howell post hoc test used to make individual pair comparisons.

Geph MFI values for $CB2_{SH3-}$ were collected from 56 transfected and 56 non-transfected neurons in 7 brain sections originating from 4 animals processed in 4 immunofluorescence experiments. The vGAT MFI values for $CB2_{SH3-}$ were collected from 24 transfected and 24 non-transfected neurons in 2 brain sections from 2 animals in 2 immunofluorescence experiments. The Geph and vGAT MFI values for $CB2_{SH3+}$ were collected from 26 transfected and 26 non-transfected neurons in 2 brain sections from 2 animals in 2 immunofluorescence experiments. Geph and vGAT cluster number and size values for $CB2_{SH3-}$ were collected from 19 transfected and 18 non-transfected neurons in 2 brain sections from 2 animals in 2 immunofluorescence experiments. Geph and vGAT cluster number and size for $CB2_{SH3+}$ were collected from 19 transfected and 19 non-transfected cells in 2 brain sections from 2 animals in 2 immunofluorescence experiments. The mIPSCs for electrophysiology were collected from 10 $CB2_{\mathbf{SH3}-}$ transfected neurons (4,197 events) from 3 IUEP animals, 9 $CB2_{\mathbf{SH3}+}$ transfected neurons (3,537 events) from 6 IUEP animals, and 10 non-transfected neurons (3,597 events) from 5 IUEP animals.

Preparation of *ex-vivo* brain slices

Ex-vivo brain slices were prepared for electrophysiology experiments from adult IUEP rats (P55-P129 rats). Rats were deeply anesthetized with isoflurane and then decapitated. Brains were rapidly removed and immersed in ice-cold oxygenated (95% O_2 and 5% CO_2) dissection buffer containing (in mM): 83 NaCl, 2.5 KCl, 1 NaH_2PO_4, 26.2 $NaHCO_3$, 0.5 $CaCl_2$, and 3.3 $MgCl_2$, 22 glucose, 72 sucrose, 300–320 mOsm, pH 7.3–7.4. Coronal slices (400 μm) were cut with a vibratome (VT1200S; Leica, Nussloch, Germany), incubated in dissection buffer for 40 min at 37°C, and then stored at room temperature for the reminder of the recording day. All slice recordings were performed at 34°C. Slices were visualized with inversion recovery differential interference microscopy (E600FN; Nikon, Tokyo, Japan) and a CCD camera (QICAM; QImaging, Surrey, British Columbia, Canada). Individual neurons were visualized with a 40x/0.8 Nikon Fluor water immersion objective.

Whole-cell patch-clamp recording

Miniature IPSCs (mIPSCs) were recorded in whole-cell voltage clamp mode using Multiclamp 700B (Molecular Devices, Sunnyvale, CA, USA), sampled at 5 kHz, digitized (ITC-18; HEKA Instruments, Bellmore, NY) and filtered at 2 kHz with an 8-pole low pass Bessel filter. Data were monitored, acquired and analyzed with Axograph X software (Berkley, CA). For all experiments, extracellular recording buffer (Artificial cerebrospinal fluid, ACSF) was oxygenated (95% O_2 and 5% CO_2) and contained (in mM): 125 NaCl, 25 $NaHCO_3$, 1.25 NaH_2PO_4, 3 KCl, 1 $MgCl_2$, and 2 $CaCl_2$, 25 glucose, pH 7.3–7.4. Patch pipettes were fabricated from borosilicate glass (N51A; King Precision Glass, Claremont, California) to a resistance of 4–8 MΩ. The resultant errors were minimized with bridge balance and capacitance compensation. Pipettes were filled with internal solution containing (in mM): 145 KCl, 10 HEPES, 5 Mg-ATP, 0.2 Na-GTP, 5 EGTA, 10 2-Tris-phosphocreatine, 0.05% biocytin, adjusted to pH 7.2–7.3 with potassium hydroxide, osmolarity 305 mOsM. Reported membrane potentials and holding potentials were not corrected for liquid junction potential. Series resistance was monitored throughout the experiments with 10 mV steps and measurement of capacitive current using Test seal routing of Axograph X. The series resistance was typically from 10–40 MΩ. The membrane potential was held at −80 mV.

AMPA and kainate receptors mediated currents were blocked by 10 μM NBQX (catalog # ab120045, Abcam plc., Cambridge, MA). NMDA mediated currents were blocked by 100 μM D-AP5 (catalog # ab120003, Abcam plc.). Glycinergic inhibitory currents were blocked by 1–2 μM Strychnine (catalog # ab120416, Abcam plc.). For mIPSCs recording, action potential evoked events were blocked by 1 μM TTX (catalog # ab120054, Abcam plc.). The recorded data of 1–5 min was analyzed at 3 min after the beginning of TTX application. To confirm the GABAergic nature of the mIPSCs, 10 μM SR-95531 $GABA_A$ receptor inhibitor (gabazine, catalog # ab120042, Abcam plc.) applied at the end of each recording blocked mIPSCs and IPSCs. The mIPSCs were identified using the semiautomatic sliding template method as previously described (Clements and Bekkers, 1997) and were visually confirmed. Origin (OriginLab, Northampton, MA; RRID:SCR_002815) and Corel Draw Graphic Suite X5 (Corel Corporation, Ottawa, Canada; RRID:SCR_013674) were used for graph generation, and SPSS (IBM Corp., Armonk, NY; RRID:SCR_002865) was used for statistical analysis.

RESULTS

Embryonic neuronal precursors that have been IUEP with $CB2_{SH3-}$ or $CB2_{SH3+}$ migrate to the appropriate layer of the cerebral cortex and overexpress $CB2_{SH3-}$ or $CB2_{SH3+}$ in the adult.

A group of E14-E15 rat embryos were co-injected (in the lateral ventricle) and co-electroporated *in utero* with HA-$CB2_{SH3-}$ and EGFP DNAs. A second group of embryos were co-electroporated with HA-$CB2_{SH3+}$ and EGFP. A third group were IUEP with EGFP only (control). At E14-E15, the neuronal precursors lining the wall of the ventricle radially migrate to their final destination in layers II-III of the cerebral cortex, differentiating into glutamatergic neurons. The neurons expressing the transfected plasmids showed normal migration and apparent normal neuronal morphology in the adult cerebral cortex (Fig 1 A–C). At P41–P45, in animals co-electroporated with EGFP and HA-$CB2_{SH3-}$ or HA-$CB2_{SH3+}$, over 95% of the neurons that expressed EGFP also co-expressed HA-$CB2_{SH3-}$ or HA-$CB2_{SH3+}$, and vice-versa, as shown by the co-localization of EGFP and anti-HA fluorescence in soma and dendrites (Fig 1D *vs.* G; F *vs.* I) and the co-localization of EGFP, anti-HA and strong anti-collybistin immunofluorescence, as shown in Fig 1J–Lfor EGFP and HA-$CB2_{SH3-}$ co-transfected neurons. In control animals in which EGFP was IUEP alone (without HA-CB2), neurons expressing EGFP did not show anti-HA immunofluorescence, Fig 1E *vs.* H) or strong CB immunofluorescence, which demonstrates the specificity of the anti-HA and anti-CB antibodies for revealing HA-$CB2_{SH3-}$ and HA-$CB2_{SH3+}$ overexpressing neurons.

In the adult cerebral cortex, neurons overexpressing $CB2_{SH3-}$ show an increase in the number, size, and fluorescence intensity of gephyrin clusters compared to controls.

At postnatal day P44–45, the age when the animals were sacrificed, the transfected neurons of the cerebral cortex that co-overexpressed $CB2_{SH3-}$ and EGFP (green, asterisks) often showed Geph clusters (blue) of significantly larger size and fluorescence intensity than neighboring non-transfected neurons ($ symbol) as shown in Fig 2A–F and Fig 7G–H. These effects could be easily appreciated by qualitative observation and are shown

quantitatively in Fig 3. The Geph superclusters were localized in both soma (arrows) and dendrites (arrowheads) of transfected neurons. Neurons from brains IUEP with EGFP only, showed Geph clusters of size and fluorescence intensity similar to that of neighboring non-transfected neurons (as shown below in Fig 7E–F). Quantification (Fig 3) shows that the transfected neurons have a significant increase (48.5%) in Geph mean fluorescence intensity/pixel (148.5 ± 7.3, mean ± SEM, Mann-Whitney U=728, $p<0.001$, $n_1=n_2=56$ neurons) normalized and compared to that of non-transfected sister neighboring neurons (100 ± 3.9). The size of Geph clusters was also significantly enhanced (74.6%) in the $CB2_{SH3-}$ overexpressing neurons (0.340 μm^2 ± 0.011, mean ± SEM, Mann-Whitney U=37,111, $p<0.0001$, $n_1=486$ clusters, $n_2=246$ clusters) compared to that of non-transfected neighbor neurons (0.195μm^2 ± 0.011). In addition, quantification revealed that the number of Geph clusters was significantly increased (86.6%) in somas of the $CB2_{SH3-}$ overexpressing neurons (27 clusters/soma ± 1.82, mean ± SEM, Mann Whitney U=38, $p<0.0001$, $n_1=18$ neurons, $n_2=17$ neurons) compared to neighboring control neurons (14.47 clusters/soma ± 1.87).

Many of the gephyrin superclusters in somas and dendrites of $CB2_{SH3-}$ overexpressing neurons are associated with presynaptic GABAergic terminals.

We tested whether the postsynaptic Geph superclusters induced by $CB2_{\mathbf{SH3}-}$ overexpression were associated with presynaptic vGAT-containing GABAergic terminals. Triple-label immunofluorescence shows (Fig 4A–F) that the Geph superclusters (blue) of transfected neurons (green, asterisk) in somas (arrows) and dendrites (arrowheads) are frequently associated with presynaptic vGAT+ puncta (red). These results indicate that the Geph superclusters present in $CB2_{\mathbf{SH3}-}$ overexpressing neurons are mostly localized at GABAergic synapses.

Postsynaptic $CB2_{SH3-}$ overexpression does not significantly affect the GABAergic innervation of these neurons.

We tested whether the formation of postsynaptic Geph superclusters had an effect on presynaptic GABAergic innervation of the transfected neurons. Triple-label immunofluorescence showed that $CB2_{\mathbf{SH3}-}$ overexpressing neurons (asterisks) did not significantly differ from neighboring non-transfected neurons (numbers 1 and 2) regarding the size, number or fluorescence intensity of the vGAT-containing presynaptic terminals (red puncta) that innervate the transfected cells, as shown by qualitative (Fig 4G–H and I–J) and quantitative analysis (Fig 5). The vGAT MFI of presynaptic terminals contacting neurons transfected with $CB2_{\mathbf{SH3}-}$ (normalized to that of non-transfected neurons) was not significantly different (103.5 ± 5.5, mean ± SEM, Mann Whitney U=263, p=0.614, $n_1=n_2=24$ neurons) from that of non-transfected sister neighboring neurons (100 ± 5.4). In addition, no significant difference was seen in either the size of vGAT clusters around the somas of $CB2_{SH3-}$ overexpressing neurons (0.3350 μm^2 ± 0.14, mean ± SEM, Mann-Whitney U=108,869, p=0.515, $n_1=496$ clusters, $n_2=450$ clusters) compared to non-transfected controls (0.320 μm^2 ± 0.14) or the number of vGAT clusters around the somas of the $CB2_{SH3-}$ overexpressing neurons (27.56 clusters/soma ± 2.894, mean ± SEM, Mann-Whitney U=136.5, p=0.597, $n_1=18$ neurons, $n_2=17$ neurons) compared to non-transfected controls (26.47 ± 3.11). These results indicate that the formation of postsynaptic Geph

superclusters in the $CB2_{SH3-}$ transfected neurons is not accompanied by a significant change in presynaptic vGAT or extent of GABAergic innervation that these neurons receive. In other words, $CB2_{SH3-}$ overexpression does not promote GABAergic synaptogenesis.

In $CB2_{SH3-}$ overexpressing neurons, $GABA_A$Rs co-localize with gephyrin superclusters.

We tested whether the postsynaptic Geph superclusters induced by $CB2_{SH3-}$ overexpression had associated $GABA_A$R clusters. Triple-label fluorescence shows that the majority of the Geph clusters (red) in the $CB2_{SH3-}$ transfected cells co-localize with $GABA_A$R clusters (blue), as revealed with an anti-γ2 $GABA_A$R antibody (arrowheads, Fig 6A–C and D–F). Quantification of 8 CB2SH3− overexpressing neurons showing Geph superclusters showed that, 94.8% of Geph clusters were colocalized with γ2 clusters (n=265 Geph clusters). In some transfected neurons, the $GABA_A$R clusters were larger than in neighbor non-transfected neurons (Fig 6D–F). The postsynaptic colocalization of γ2 $GABA_A$Rs with Geph and the apposition of vGAT puncta shown above, indicate that the GABAergic superclusters induced by $CB2_{SH3-}$ correspond to functional synapses. We have confirmed that this is indeed the case with the electrophysiology experiments described below.

$CB2_{SH3+}$ overexpression in vivo has a smaller but still enhancing effect on gephyrin clustering.

Qualitative analysis (Fig 7A–B and C–D) shows that in the cerebral cortex of P41–P42 IUEP rats, neurons that co-overexpress $CB2_{SH3+}$ and EGFP (green, asterisks) had Geph clusters (blue) of similar size and fluorescence intensity to those of non-transfected sister neighboring neurons ($ symbol) or to those neurons from rats that were IUEP with EGFP only (Fig 7E–F). Quantification (Fig 8) shows that the $CB2_{SH3+}$ overexpressing neurons have a slight but significant increase (11%) in mean Geph fluorescence intensity/pixel (111.1± 3.6, mean ± SEM, Mann Whitney U=224, p=0.038, $n_1=n_2=26$ neurons) normalized and compared to that of non-transfected neurons (100 ±3.8). Similarly, quantification of Geph cluster size showed that there was a small but significant increase (11.9%) in the size of Geph clusters in $CB2_{SH3+}$ overexpressing neurons (0.249 μm^2 ± 0.009, mean ± SEM, Mann Whitney U=74,346, p=0.039, n_1=433 clusters, n_2=375 clusters) compared to non-transfected control neurons (0.223μm^2 ± 0.009) In addition, there was a slight increase (15.5%) in the number of Geph clusters in the somas of the $CB2_{SH3+}$ overexpressing neurons (24.06 clusters/soma ± 1.45, mean ± SEM) compared to non-transfected controls (20.83 clusters/soma ± 1.16); however, this difference was not statistically significant (Mann Whitney U=112, p=0.117, $n_1=n_2=18$ neurons, Fig 8).

Fig 7G–H depicts the formation of Geph superclusters in a $CB2_{SH3-}$ and EGFP co-expressing neuron for comparison with the Geph clusters in neurons co-expressing $CB2_{SH3+}$ and EGFP.

Many of the gephyrin clusters in somas and dendrites of $CB2_{SH3+}$ overexpressing neurons are associated with presynaptic GABAergic terminals.

Triple-label immunofluorescence shows (Fig 9A–C and D–F) that in the $CB2_{SH3+}$ transfected neurons (green, asterisk), and in the non-transfected neighboring neurons (*i.e.* neuron 1), the Geph clusters (blue) are frequently associated with presynaptic vGAT+ puncta

(red) in the soma (arrows) and dendrites (arrowheads), indicating that these Geph clusters in $CB2_{\mathbf{SH3+}}$ overexpressing neurons, as in non-transfected neurons, are frequently localized at GABAergic synapses.

Qualitative analysis shows that the vGAT+ puncta associated with $CB2_{\mathbf{SH3+}}$ overexpressing neurons were not significantly different (in size, number or fluorescence intensity) from that of non-transfected sister neurons (Fig 9A–C and G–H). Quantification in Fig 10 also showed no significant difference in vGAT mean fluorescence intensity between $CB2_{\mathbf{SH3+}}$ transfected neurons (98.8± 3.5, mean ± SEM, Mann-Whitney U=336, p=0.963, $n_1=n_2=26$ neurons) and neighboring non-transfected neurons (100±3.2). In addition, no significant differences were found in the size of vGAT clusters around the $CB2_{SH3+}$ overexpressing neurons (0.597μm^2 ± 0.029, mean ± SEM, Mann-Whitney U=65,058, p=0.297, n_1=368 clusters, n_2=372 clusters) compared to non-transfected controls (0.640 μm^2 ± 0.03) or the number of vGAT clusters around $CB2_{SH3+}$ overexpressing somas (20.39 clusters/soma ± 1.01, mean ±SEM, Mann-Whitney U=158.5, p=0.924, $n_1=n_2=19$ neurons) compared to non-transfected controls (20.61 clusters/soma ± 1.09). These results indicate that $CB2_{\mathbf{SH3+}}$ overexpression in neurons has no significant effect on the GABAergic innervation that these neurons receive.

Pyramidal neurons overexpressing $CB2_{\mathbf{SH3-}}$ or $CB2_{\mathbf{SH3+}}$ show a significant increase in the amplitude of GABAergic mIPSCs

We have measured mIPSCs amplitude in pyramidal neurons of layers II-III of the adult somatosensory cerebral cortex of rats that had been IUEP with $CB2_{\mathbf{SH3-}}$ (plus EGFP) or with $CB2_{\mathbf{SH3+}}$ (plus EGFP) expression plasmids. For these experiments we did whole-cell voltage-clamp *ex-vivo* recording in slices from adult brains of IUEP animals (Chen and LoTurco, 2012; Tabata and Nakajima, 2001). Neurons overexpressing $CB2_{\mathbf{SH3-}}$ show mIPSCs of larger amplitude than non-transfected neurons or neurons transfected with $CB2_{\mathbf{SH3+}}$ (Fig 11A–B). There is a right shift in the cumulative probability of the mIPSC amplitude in the neurons overexpressing $CB2_{\mathbf{SH3-}}$ compared to neurons overexpressing $CB2_{\mathbf{SH3+}}$ or to non-transfected neurons (Kolmogorov-Smirnov (K-S) test p<0.001 in both cases). There is also a higher proportion of large amplitude mIPSCs in neurons transfected with $CB2_{\mathbf{SH3-}}$ compared to non-transfected neurons or neurons transfected with $CB2_{\mathbf{SH3+}}$ (Fig 11C).

The average amplitude of $GABA_AR$ mediated mIPSCs (mean ± SEM) was significantly larger in pyramidal cells overexpressing $CB2_{\mathbf{SH3-}}$ (25.72 ± 0.33 pA) than in either non-transfected neighbor pyramidal cells (19.38 ± 0.18 pA) or pyramidal cells overexpressing $CB2_{\mathbf{SH3+}}$ (21.57 ±0.29 pA) as shown in Fig 11D. The same results also show (Fig 11D) that the average mIPSC amplitude in pyramidal cells overexpressing $CB2_{\mathbf{SH3+}}$ was significantly larger than in non-transfected neighbor pyramidal cells (Welch ANOVA F=142.42, p<0.0001, n=4,197 events for $CB2_{SH3-}$, 3,537 events for CB2SH3+, and 3,597 events from non-transfected neurons, Games-Howell post-hoc test non-transfected to $CB2_{\mathbf{SH3-}}$ q= 6.34, p<0.001, $CB2_{\mathbf{SH3+}}$ to $CB2_{\mathbf{SH3-}}$ q=4.15, p<0.001, non-transfected to $CB2_{\mathbf{SH3+}}$ q= 2.19, p<0.001).

Pyramidal neurons overexpressing either $CB2_{SH3-}$ or $CB2_{SH3+}$ show a significant decrease in the frequency of GABAergic mIPSCs

The inter-event interval cumulative probability curve in either $CB2_{SH3-}$ or $CB2_{SH3+}$ transfected neurons was shifted to the right (Fig 11E). There is a significant difference between non-transfected cells compared to either $CB2_{SH3-}$ or $CB2_{SH3+}$ transfected cells ($p<0.001$ in K-S test). Non-transfected pyramidal cells had higher mIPSC instantaneous frequency (15.25 ± 0.21 Hz, mean ± SEM, $p<0.001$) than neurons overexpressing $CB2_{SH3-}$ (12.11 ±0.21 Hz) or $CB2_{SH3+}$ (11.97 ± 0.22 Hz), as shown in Fig 11F. Pyramidal neurons transfected with either $CB2_{SH3-}$ or $CB2_{SH3+}$ showed no significant difference in inter-event interval or instantaneous frequency (Welch ANOVA $F=75.74$, $p<0.0001$, n=4,197 events for $CB2_{SH3-}$, 3,537 events for CB2SH3+, and 3,597 events from non-transfected neurons, Games-Howell post-hoc test non-transfected to $CB2_{SH3-}$ $q=3.13$, $p<0.001$, $CB2_{SH3+}$ to $CB2_{SH3-}$ $q=0.15$, $p=0.876$, non-transfected to $CB2_{SH3+}$ $q=3.28$, $p<0.001$, Fig 11E–F).

DISCUSSION

In this communication, we have studied the effect on GABAergic synapses of chronic *in vivo* overexpression of $CB2_{SH3-}$ or $CB2_{SH3+}$, in neurons of the adult rat cerebral cortex after IUEP. To the best of our knowledge these are the first studies of collybistin overexpression in the brain.

Effects of *in vivo* $CB2_{SH3-}$ overexpression on GABAergic synapses

Overexpression of $CB2_{SH3-}$ (and EGFP) in neurons of the rat cerebral cortex led to the formation of significantly larger and/or brighter postsynaptic Geph clusters in these neurons (superclusters) than in the non-transfected sister neurons or neurons transfected with EGFP only. Quantification showed a significant increase in mean Geph fluorescence intensity/pixel over non-transfected neurons (48.5% $p<0.0001$). As well as a significant increase in the size (74.6%) and number (86.6%) of Geph clusters in the somas of these neurons. Many of the superclusters were apposed to vGAT+ presynaptic terminals indicating that these Geph and $GABA_AR$ superclusters were frequently localized at GABAergic synapses. This notion is also supported by the observed significant increase (33%) in the amplitude of mIPSCs, in the $CB2_{SH3-}$ overexpressing pyramidal cells over non-transfected pyramidal cells. The increase in mIPSC amplitude is interpreted as an increase in the density of functional postsynaptic $GABA_ARs$, which is consistent with increased size and/or fluorescence intensity of postsynaptic Geph (superclusters) and $GABA_ARs$ in the GABAergic synapses that the $CB2_{SH3-}$ overexpressing neurons receive.

The $CB2_{SH3-}$ overexpressing neurons showed no apparent effect on the fluorescence intensity, number, or size of vGAT puncta contacting them over neighboring non-transfected neurons. However, the frequency of mIPSCs in the $CB2_{SH3-}$ overexpressing neurons was decreased 22% compared to non-transfected neighboring neurons. The lack of effect on vGAT and the decreased mIPSC frequency together suggest that the number of synaptic contacts does not change but the probability of spontaneous vesicular presynaptic GABA release is decreased (as discussed below).

Effects of *in vivo* $CB2_{SH3+}$ overexpression on GABAergic synapses

Qualitative analysis showed that neurons overexpressing $CB2_{SH3+}$ had no apparent effect on the size or fluorescence intensity of postsynaptic Geph clusters compared to non-transfected sister neurons. However, quantification showed a small but significant increase in mean Geph mean fluorescence intensity/pixel over non-transfected neurons (11.1 % increase, p=0.038) as well as Geph cluster size (11.9% p=0.039). The Geph clusters in the transfected neurons corresponded to GABAergic synapses because they were frequently apposed to vGAT+ presynaptic terminals. Consistent with these results, the mIPSCs of the $CB2_{SH3+}$ overexpressing pyramidal cells had slightly but significant larger amplitude (11% $p<0.001$) than non-transfected sister neurons, suggesting that the GABAergic synapses in these neurons have slightly higher number of postsynaptic $GABA_A$Rs than non-transfected neurons. The results show that although the effect is significantly smaller than with $CB2_{SH3-}$, the overexpression of $CB2_{SH3+}$ also induces a significant increase in postsynaptic clustering and mIPSC amplitude.

There was no apparent effect on the mean fluorescence intensity/pixel size, or number of vGAT+ puncta contacting the $CB2_{SH3+}$ overexpressing neurons compared to non-transfected neurons. In $CB2_{SH3+}$ overexpressing neurons, the mIPSCs frequency was decreased 22%, however, there was no change in vGAT puncta. The results are consistent with a decreased probability of spontaneous vesicular GABA release from the presynaptic GABAergic terminals contacting $CB2_{SH3+}$ overexpressing neurons (as discussed below).

Differences in the experimental design between acute CB overexpression in neuronal cultures and chronic overexpression *in vivo*

In our previous studies on HP neuronal cultures (Chiou et al., 2011), the expression of CB was acute. Transfections were done at 10DIV and the assay for Geph and $GABA_A$R cluster formation was done at 13DIV. In the present communication, transfections of neuronal embryonic precursors were done *in utero*. Transfected neurons migrated to the appropriate cortical layer and CB was chronically overexpressed in these neurons for weeks after birth. The synaptic effects were assessed in adulthood in transfected neurons that became developmentally and functionally integrated in circuits of the cerebral cortex. It is also worth mentioning that in our earlier studies we transfected cultured neurons from hippocampus while in the *in vivo* experiments here, we transfected neurons in the cerebral cortex. Nevertheless, others have shown that large Geph clusters also form in cultured neurons from cerebral cortex after acute CB overexpression (Kalscheuer et al., 2009).

In spite of these experimental differences there were some similarities with the *in vitro* results. The *in vivo* overexpression of $CB2_{SH3-}$ after IUEP led to the formation of Geph and $GABA_A$R superclusters in the transfected cortical neurons and to a significant increase in the amplitude of their mIPSCs, as we found *in vitro* (Chiou et al., 2011).

We tested whether Geph superclusters were also present in older (P165) rats that were IUEP with $CB2_{SH3-}$. Preliminary qualitative data indicates that Geph superclusters are present in the soma and dendrites of older (P165) rats that were IUEP with $CB2_{SH3-}$ (not shown), suggesting that *in vivo*, CB overexpression effects are long lasting.

Significant differences in the results between the *in vivo* and in culture experiments.

There are significant differences in the results obtained with the two experimental approaches. In HP cultures we found no significant effect of $CB2_{\mathbf{SH3}-}$ overexpression on mIPSC frequency (only in mIPSC amplitude). In contrast, *in vivo* we found a significant decrease (22%) in mIPSC frequency, likely corresponding to a decrease probability of GABA release since there is no effect on the number of vGAT-containing synaptic contacts. One possible explanation is a transynaptic effect from the transfected neuron to the presynaptic terminal resulting in reduced probability of spontaneous synaptic vesicle release. Alternatively, the presynaptic effect could be due to a homeostatic plasticity mechanism by which long-term increased synaptic inhibition of the pyramidal cells results in decreased activation of interneurons by the axon collaterals from pyramidal cells, in turn resulting in long-term decreased probability of GABAergic synaptic vesicle release. These circuit mechanisms might be absent in neuronal cultures.

Also, significant differences with the *in vitro* results were found in neurons overexpressing $CB2_{\mathbf{SH3}+}$. *In vivo* overexpression of $CB2_{\mathbf{SH3}+}$ increases both Geph clustering (by 11%, $p=0.038$) and the amplitude of mIPSCs (by 11%, $p<0.001$), indicating an enhancing effect of $CB2_{\mathbf{SH3}+}$ in postsynaptic Geph and $GABA_AR$ number. In contrast, *in vitro* $CB2_{\mathbf{SH3}+}$ showed no significant synaptic effects.

We also observed that *in vivo*, the pyramidal neurons overexpressing $CB2_{\mathbf{SH3}+}$, showed decreased (21%) mIPSC frequency, while in vitro there was no effect on frequency. Therefore, the *in vivo* overexpression of either $CB2_{\mathbf{SH3}-}$ or $CB2_{\mathbf{SH3}+}$ leads in both cases to enhanced Geph clustering, increased mIPSC amplitude and decreased mIPSC frequency.

In the hippocampus of the CB-deficient mouse there was a reduction of mIPSC amplitude and frequency (Papadopoulos et al., 2007). These results could be explained entirely by postsynaptic mechanisms. The decrease in mIPSC frequency could result from failure to detect all single synaptic vesicle spontaneous GABA release events due to decreased postsynaptic $GABA_ARs$ and $GABA_AR$ clusters in the CB K.O. mouse. These mice showed no reduced number of presynaptic vGAT puncta. In our experiments, the observed decrease in mIPSC frequency cannot be attributed to a postsynaptic mechanism, because there is an increase in mIPSC amplitude. If anything, it would be accompanied by an increase mIPSC frequency, not a reduction. Therefore, the most likely explanation for our results is presynaptic as discussed above. Another significant difference is that *in vivo*, the large majority of the Geph clusters in the $CB2_{\mathbf{SH3}+}$ overexpressing neurons were synaptic, while *in vitro*, they were mostly extrasynaptic. The results show that many of the *in vitro* results cannot be extrapolated to *in vivo*.

CB regulates Geph/$GABA_AR$ clustering in both cerebral cortex and hippocampus.

The CB-deficient mice show reduced Geph/$GABA_AR$ clustering and impaired GABAergic transmission in the hippocampus and amygdala but little or no effect on the cerebral cortex (Papadopoulos et al., 2008; Papadopoulos et al., 2007). Nevertheless, the Geph/$GABA_AR$ clustering-promoting effect of CB occurs in cortical neurons both *in vivo,* as reported in this communication, and in cultured cortical neurons (Kalscheuer et al. 2009) as well as in

cultured HP neurons (Chiou et al., 2011; Papadopoulos et al., 2015; Soykan et al., 2014; Tyagarajan et al., 2011). Thus, although CB is not essential in cerebral cortex for GABAergic synapse formation or maintenance, (likely due to the existence of redundant mechanisms), CB expression can regulate the strength of GABAergic synapses in both hippocampus and cerebral cortex. Our results are consistent with the documented expression of CB mRNA and protein not only in hippocampus and amygdala, but also in cerebral cortex (and in many GABAergic synapse of the cerebral cortex) and other brain regions (Kins et al., 2000; Patrizi et al., 2012).

CB regulates Geph/GABA$_A$R clustering in both soma and dendrites.

There is evidence of differential molecular mechanisms for the assembly of GABAergic postsynaptic elements in the soma *vs.* dendrites (Frola et al., 2013; Jedlicka et al., 2011; Panzanelli et al., 2011; Poulopoulos et al., 2009). Our results (Fig 2) show that CB2$_{\mathbf{SH3}-}$ overexpression leads to the formation of Geph/GABA$_A$R superclusters both in the soma and dendrites suggesting that these differences in clustering between soma and dendrites are not due to CB. This notion is also supported by the studies on the CB-deficient mouse which show that the postsynaptic clustering of Geph and GABA$_A$R was disrupted both in soma and dendrites (Papadopoulos et al., 2008; Papadopoulos et al., 2007).

Differences between the *in vivo* gephyrin/GABA$_A$R clustering effects of CB2$_{\mathbf{SH3-}}$ and CB2$_{\mathbf{SH3+}}$

As described above, *in vivo* overexpression of CB2$_{\mathbf{SH3}-}$ leads to synaptic Geph superclustering compared to the much smaller effect in Geph clustering induced by the overexpression of CB2$_{\mathbf{SH3}+}$. Nevertheless, little is known about the possible differential functional roles of CB$_{\mathbf{SH3}-}$ and CB$_{\mathbf{SH3}+}$ isoforms in GABAergic synapses *in vivo*. In co-transfected HEK293 or COS-7 cells, the constitutively active CB$_{\mathbf{SH3}-}$ isoforms induce the accumulation of submembranous Geph clusters while CB$_{\mathbf{SH3}+}$ isoforms have to be activated in order to induce the formation of submembranous Geph clusters (Harvey et al., 2004; Kalscheuer et al., 2009; Kins et al., 2000; Papadopoulos et al., 2015; Soykan et al., 2014). The SH3 domain of CB2$_{\mathbf{SH3}+}$ exerts an auto-inhibitory effect on the PH domain. In co-transfected HEK293 cells, neuroligin 2 (NL2) binds to the SH3 domain of CB$_{\mathbf{SH3}+}$ releasing the autoinhibition of CB, activating it and inducing the formation of submembranous Geph clusters (Hoon et al., 2011; Papadopoulos et al., 2015; Poulopoulos et al., 2009; Soykan et al., 2014). Based on these results with HEK293 cells, and the selective localization of NL2 in GABAergic synapses, it has been proposed that at the onset of GABAergic synapse formation, the activation of CB$_{\mathbf{SH3}+}$ by the synaptically localized NL2 leads to Geph and GABA$_A$R accumulation at the postsynapse (Poulopoulos et al., 2009; Saiepour et al., 2010; Soykan et al., 2014). However, in cultured HP neurons of NL2−/− mouse mutants, CB2$_{\mathbf{SH3}-}$ overexpression also induces the superclustering of Geph at GABAergic synapses (Soykan et al., 2014), indicating that NL2 is dispensable in the tethering of Geph and CB to the GABAergic postsynapse and that there are also NL2-independent tethering mechanisms involved in the postsynaptic accumulations of Geph and GABA$_A$Rs. Also NL4, as NL2 does, binds to CB$_{\mathbf{SH3}+}$ activating it (Hoon et al., 2011). It has been proposed that NL4 compensates for the loss of NL2 in NL2−/− mouse mutant at GABAergic synapses (Hoon et al., 2011). Although this might occur in the retina, it has not been shown to be the case in

brain although there is a compensatory upregulation of the NL2/NL1 ratio in the hippocampus of the NL4 KO mouse (Hammer et al., 2015). In addition, the large intracellular loop (IL) of the $GABA_AR$ α2 subunit (α2IL) also binds to the SH3 domain, activating CB_{SH3+} in HEK293 cells (Saiepour et al., 2010). The small rho GTPase TC10 also activates CB_{SH3+} by interacting with the PH domain itself (Mayer et al., 2013; Papadopoulos et al., 2015). Nevertheless, there is no evidence that any of these CB-activation mechanisms operate in neurons or GABAergic synapses. Although in the rat brain as a whole, there is considerably higher expression of CB_{SH3+} than CB_{SH3-} mRNA (Harvey et al., 2004), CB_{SH3+} is self-inhibited while CB_{SH3-} is constitutively active (Harvey et al., 2004; Kins et al., 2000; Ludolphs et al., 2016; Papadopoulos et al., 2015). Thus, fewer molecules of CB_{SH3-} could have a strong functional role, particularly if they concentrate in certain brain regions or neurons. Therefore, the possible differential functional roles of endogenous CB_{SH3-} and CB_{SH3+} isoforms are not understood.

Postsynaptic clustering of $GABA_ARs$ regulates the strength and plasticity of inhibitory synapses and maintains the excitation/inhibition balance in the brain (Fritschy and Panzanelli, 2014; Luscher et al., 2011). Our results show that we can significantly enhance both the postsynaptic clustering of $GABA_ARs$ and mIPSCs amplitude of GABAergic inhibitory synapses *in vivo* by transgenic overexpression of CB. The excitation/inhibition (E/I) balance is disrupted in several neurological and mental disorders including epilepsy, anxiety, depression, schizophrenia, autism, sleep disorders and hyperekplexia among others (Bourgeron, 2009; Zoghbi, 2003). In several of these diseases pathological impairment of inhibitory synapses has been described (Charych et al., 2009; Harvey et al., 2008; Kalscheuer et al., 2009; Lemke et al., 2012; Lesca et al., 2011; Marco et al., 2008; Pizzarelli and Cherubini, 2011; Rudolph and Mohler, 2013; Shimojima et al., 2011). Thus, a possible strategy for ameliorating some symptoms of these diseases could be based on the controlled manipulation of CB function aimed to restore the E/I balance.

AKCNOWLEDGEMENTS

We thank Profs. Robert J. Harvey and Kirsten Harvey (UCL school of pharmacy, London) for providing the cmyc-$CB2_{SH3+}$ and cmyc-$CB2_{SH3-}$ plasmids. We also thank Rachel S. Harris and David Ahearn Jr. for their help in setting up some of the conditions for the immunofluorescence experiments. This research was supported by the NIH/NICHD grants P01HD055655 and P01HD057853 to J.J.L. and the NIH/NIND grant R01NS038752 to A.L.D.

ABBREVIATIONS:

aa	amino acids
CB	collybistin
GABA	γ-aminobutyric acid
$GABA_AR$	γ-aminobutyric acid type A receptor
GEF	guanine nucleotide exchange factor
Geph	gephyrin
GP	guinea pig

HA	human influenza hemagglutinin
HP	hippocampal
IUEP	*in utero* electroporation
mAb	monoclonal antibody
MFI	mean fluorescence intensity
mIPSC	miniature inhibitory postsynaptic current
Ms	mouse
NGS	normal goat serum
NL	neuroligin
PB	phosphate buffer
Rb	rabbit
RT	room temperature
SH3	*src* homology 3 domain
vGAT	vesicular GABA transporter
vGLUT1	vesicular glutamate transporter 1

LITERATURE CITED

Bai J, Ramos RL, Ackman JB, Thomas AM, Lee RV, LoTurco JJ. 2003. RNAi reveals doublecortin is required for radial migration in rat neocortex. Nat Neurosci 6(12):1277–1283. [PubMed: 14625554]

Bourgeron T 2009. A synaptic trek to autism. Current opinion in neurobiology 19(2):231–234. [PubMed: 19545994]

Charych EI, Liu F, Moss SJ, Brandon NJ. 2009. GABA(A) receptors and their associated proteins: implications in the etiology and treatment of schizophrenia and related disorders. Neuropharmacology 57(5–6):481–495. [PubMed: 19631671]

Charych EI, Yu W, Li R, Serwanski DR, Miralles CP, Li X, Yang BY, Pinal N, Walikonis R, De Blas AL. 2004a. A four PDZ domain-containing splice variant form of GRIP1 is localized in GABAergic and glutamatergic synapses in the brain. J Biol Chem 279(37):38978–38990. [PubMed: 15226318]

Charych EI, Yu W, Miralles CP, Serwanski DR, Li X, Rubio M, De Blas AL. 2004b. The brefeldin A-inhibited GDP/GTP exchange factor 2, a protein involved in vesicular trafficking, interacts with the beta subunits of the GABA receptors. J Neurochem 90(1):173–189. [PubMed: 15198677]

Chen F, LoTurco J. 2012. A method for stable transgenesis of radial glia lineage in rat neocortex by piggyBac mediated transposition. J Neurosci Methods 207(2):172–180. [PubMed: 22521325]

Chiou TT, Bonhomme B, Jin H, Miralles CP, Xiao H, Fu Z, Harvey RJ, Harvey K, Vicini S, De Blas AL. 2011. Differential regulation of the postsynaptic clustering of gamma-aminobutyric acid type A (GABAA) receptors by collybistin isoforms. J Biol Chem 286(25):22456–22468. [PubMed: 21540179]

Christie SB, De Blas AL. 2003. GABAergic and glutamatergic axons innervate the axon initial segment and organize GABA(A) receptor clusters of cultured hippocampal pyramidal cells. J Comp Neurol 456(4):361–374. [PubMed: 12532408]

Christie SB, Li RW, Miralles CP, Riquelme R, Yang BY, Charych E, Wendou Y, Daniels SB, Cantino ME, De Blas AL. 2002a. Synaptic and extrasynaptic GABAA receptor and gephyrin clusters. Prog Brain Res 136:157–180. [PubMed: 12143379]

Christie SB, Li RW, Miralles CP, Yang BY, De Blas AL. 2006. Clustered and non-clustered GABAA receptors in cultured hippocampal neurons. Mol Cell Neurosci 31(1):1–14. [PubMed: 16181787]

Christie SB, Miralles CP, De Blas AL. 2002b. GABAergic innervation organizes synaptic and extrasynaptic GABAA receptor clustering in cultured hippocampal neurons. J Neurosci 22(3):684–697. [PubMed: 11826098]

Clements JD, Bekkers JM. 1997. Detection of spontaneous synaptic events with an optimally scaled template. Biophys J 73(1):220–229. [PubMed: 9199786]

Fekete CD, Chiou TT, Miralles CP, Harris RS, Fiondella CG, Loturco JJ, De Blas AL. 2015. In vivo clonal overexpression of neuroligin 3 and neuroligin 2 in neurons of the rat cerebral cortex: Differential effects on GABAergic synapses and neuronal migration. J Comp Neurol 523(9):1359–1378. [PubMed: 25565602]

Fritschy JM, Panzanelli P. 2014. GABAA receptors and plasticity of inhibitory neurotransmission in the central nervous system. Eur J Neurosci 39(11):1845–1865. [PubMed: 24628861]

Fritschy JM, Panzanelli P, Tyagarajan SK. 2012. Molecular and functional heterogeneity of GABAergic synapses. Cell Mol Life Sci 69(15):2485–2499. [PubMed: 22314501]

Frola E, Patrizi A, Goetz T, Medrihan L, Petrini EM, Barberis A, Wulff P, Wisden W, Sassoe-Pognetto M. 2013. Synaptic competition sculpts the development of GABAergic axo-dendritic but not perisomatic synapses. PloS one 8(2):e56311. [PubMed: 23457547]

Grosskreutz Y, Hermann A, Kins S, Fuhrmann JC, Betz H, Kneussel M. 2001. Identification of a gephyrin-binding motif in the GDP/GTP exchange factor collybistin. Biol Chem 382(10):1455–1462. [PubMed: 11727829]

Hammer M, Krueger-Burg D, Tuffy LP, Cooper BH, Taschenberger H, Goswami SP, Ehrenreich H, Jonas P, Varoqueaux F, Rhee JS, Brose N. 2015. Perturbed Hippocampal Synaptic Inhibition and gamma-Oscillations in a Neuroligin-4 Knockout Mouse Model of Autism. Cell Rep 13(3):516–523. [PubMed: 26456829]

Harvey K, Duguid IC, Alldred MJ, Beatty SE, Ward H, Keep NH, Lingenfelter SE, Pearce BR, Lundgren J, Owen MJ, Smart TG, Luscher B, Rees MI, Harvey RJ. 2004. The GDP-GTP exchange factor collybistin: an essential determinant of neuronal gephyrin clustering. J Neurosci 24(25):5816–5826. [PubMed: 15215304]

Harvey RJ, Topf M, Harvey K, Rees MI. 2008. The genetics of hyperekplexia: more than startle! Trends Genet 24(9):439–447. [PubMed: 18707791]

Hoon M, Soykan T, Falkenburger B, Hammer M, Patrizi A, Schmidt KF, Sassoe-Pognetto M, Lowel S, Moser T, Taschenberger H, Brose N, Varoqueaux F. 2011. Neuroligin-4 is localized to glycinergic postsynapses and regulates inhibition in the retina. Proc Natl Acad Sci U S A 108(7):3053–3058. [PubMed: 21282647]

Jedlicka P, Hoon M, Papadopoulos T, Vlachos A, Winkels R, Poulopoulos A, Betz H, Deller T, Brose N, Varoqueaux F, Schwarzacher SW. 2011. Increased dentate gyrus excitability in neuroligin-2-deficient mice in vivo. Cereb Cortex 21(2):357–367. [PubMed: 20530218]

Jin H, Chiou TT, Serwanski DR, Miralles CP, Pinal N, De Blas AL. 2014. RNF34 interacts with and promotes gamma-aminobutyric acid type-A receptor degradation via ubiquitination of the gamma2 subunit. J Biol Chem.

Kalscheuer VM, Musante L, Fang C, Hoffmann K, Fuchs C, Carta E, Deas E, Venkateswarlu K, Menzel C, Ullmann R, Tommerup N, Dalpra L, Tzschach A, Selicorni A, Luscher B, Ropers HH, Harvey K, Harvey RJ. 2009. A balanced chromosomal translocation disrupting ARHGEF9 is associated with epilepsy, anxiety, aggression, and mental retardation. Hum Mutat 30(1):61–68. [PubMed: 18615734]

Kins S, Betz H, Kirsch J. 2000. Collybistin, a newly identified brain-specific GEF, induces submembrane clustering of gephyrin. Nat Neurosci 3(1):22–29. [PubMed: 10607391]

Lemke JR, Riesch E, Scheurenbrand T, Schubach M, Wilhelm C, Steiner I, Hansen J, Courage C, Gallati S, Burki S, Strozzi S, Simonetti BG, Grunt S, Steinlin M, Alber M, Wolff M, Klopstock T, Prott EC, Lorenz R, Spaich C, Rona S, Lakshminarasimhan M, Kroll J, Dorn T, Kramer G,

Synofzik M, Becker F, Weber YG, Lerche H, Bohm D, Biskup S. 2012. Targeted next generation sequencing as a diagnostic tool in epileptic disorders. Epilepsia 53(8):1387–1398. [PubMed: 22612257]

Lesca G, Till M, Labalme A, Vallee D, Hugonenq C, Philip N, Edery P, Sanlaville D. 2011. De novo Xq11.11 microdeletion including ARHGEF9 in a boy with mental retardation, epilepsy, macrosomia, and dysmorphic features. Am J Med Genet A 155A(7):1706–1711. [PubMed: 21626670]

Li RW, Yu W, Christie S, Miralles CP, Bai J, Loturco JJ, De Blas AL. 2005. Disruption of postsynaptic GABA receptor clusters leads to decreased GABAergic innervation of pyramidal neurons. J Neurochem 95(3):756–770. [PubMed: 16248887]

Li X, Serwanski DR, Miralles CP, Bahr BA, De Blas AL. 2007. Two pools of Triton X-100-insoluble GABA(A) receptors are present in the brain, one associated to lipid rafts and another one to the post-synaptic GABAergic complex. J Neurochem 102(4):1329–1345. [PubMed: 17663755]

Li X, Serwanski DR, Miralles CP, Nagata K, De Blas AL. 2009. Septin 11 is present in GABAergic synapses and plays a functional role in the cytoarchitecture of neurons and GABAergic synaptic connectivity. J Biol Chem 284(25):17253–17265. [PubMed: 19380581]

Li Y, Serwanski DR, Miralles CP, Fiondella CG, Loturco JJ, Rubio ME, De Blas AL. 2010. Synaptic and nonsynaptic localization of protocadherin-gammaC5 in the rat brain. J Comp Neurol 518(17):3439–3463. [PubMed: 20589908]

Li Y, Xiao H, Chiou TT, Jin H, Bonhomme B, Miralles CP, Pinal N, Ali R, Chen WV, Maniatis T, De Blas AL. 2012. Molecular and functional interaction between protocadherin-gammaC5 and GABAA receptors. J Neurosci 32(34):11780–11797. [PubMed: 22915120]

Ludolphs M, Schneeberger D, Soykan T, Schafer J, Papadopoulos T, Brose N, Schindelin H, Steinem C. 2016. Specificity of Collybistin-Phosphoinositide Interactions: IMPACT OF THE INDIVIDUAL PROTEIN DOMAINS. J Biol Chem 291(1):244–254. [PubMed: 26546675]

Luscher B, Fuchs T, Kilpatrick CL. 2011. GABAA receptor trafficking-mediated plasticity of inhibitory synapses. Neuron 70(3):385–409. [PubMed: 21555068]

Machado CO, Griesi-Oliveira K, Rosenberg C, Kok F, Martins S, Rita Passos-Bueno M, Sertie AL. 2015. Collybistin binds and inhibits mTORC1 signaling: a potential novel mechanism contributing to intellectual disability and autism. Eur J Hum Genet.

Marco EJ, Abidi FE, Bristow J, Dean WB, Cotter P, Jeremy RJ, Schwartz CE, Sherr EH. 2008. ARHGEF9 disruption in a female patient is associated with X linked mental retardation and sensory hyperarousal. J Med Genet 45(2):100–105. [PubMed: 17893116]

Mayer S, Kumar R, Jaiswal M, Soykan T, Ahmadian MR, Brose N, Betz H, Rhee JS, Papadopoulos T. 2013. Collybistin activation by GTP-TC10 enhances postsynaptic gephyrin clustering and hippocampal GABAergic neurotransmission. Proc Natl Acad Sci U S A 110(51):20795–20800. [PubMed: 24297911]

Panzanelli P, Gunn BG, Schlatter MC, Benke D, Tyagarajan SK, Scheiffele P, Belelli D, Lambert JJ, Rudolph U, Fritschy JM. 2011. Distinct mechanisms regulate GABAA receptor and gephyrin clustering at perisomatic and axo-axonic synapses on CA1 pyramidal cells. J Physiol 589(Pt 20):4959–4980. [PubMed: 21825022]

Papadopoulos T, Eulenburg V, Reddy-Alla S, Mansuy IM, Li Y, Betz H. 2008. Collybistin is required for both the formation and maintenance of GABAergic postsynapses in the hippocampus. Mol Cell Neurosci 39(2):161–169. [PubMed: 18625319]

Papadopoulos T, Korte M, Eulenburg V, Kubota H, Retiounskaia M, Harvey RJ, Harvey K, O'Sullivan GA, Laube B, Hulsmann S, Geiger JR, Betz H. 2007. Impaired GABAergic transmission and altered hippocampal synaptic plasticity in collybistin-deficient mice. Embo J 26(17):3888–3899. [PubMed: 17690689]

Papadopoulos T, Schemm R, Grubmuller H, Brose N. 2015. Lipid binding defects and perturbed synaptogenic activity of a Collybistin R290H mutant that causes epilepsy and intellectual disability. J Biol Chem 290(13):8256–8270. [PubMed: 25678704]

Patrizi A, Viltono L, Frola E, Harvey K, Harvey RJ, Sassoe-Pognetto M. 2012. Selective localization of collybistin at a subset of inhibitory synapses in brain circuits. J Comp Neurol 520(1):130–141. [PubMed: 21681748]

Pfeiffer F, Simler R, Grenningloh G, Betz H. 1984. Monoclonal antibodies and peptide mapping reveal structural similarities between the subunits of the glycine receptor of rat spinal cord. Proc Natl Acad Sci U S A 81(22):7224–7227. [PubMed: 6095276]

Pizzarelli R, Cherubini E. 2011. Alterations of GABAergic signaling in autism spectrum disorders. Neural Plast 2011:297153. [PubMed: 21766041]

Poulopoulos A, Aramuni G, Meyer G, Soykan T, Hoon M, Papadopoulos T, Zhang M, Paarmann I, Fuchs C, Harvey K, Jedlicka P, Schwarzacher SW, Betz H, Harvey RJ, Brose N, Zhang W, Varoqueaux F. 2009. Neuroligin 2 drives postsynaptic assembly at perisomatic inhibitory synapses through gephyrin and collybistin. Neuron 63(5):628–642. [PubMed: 19755106]

Ramos RL, Bai J, LoTurco JJ. 2006. Heterotopia formation in rat but not mouse neocortex after RNA interference knockdown of DCX. Cereb Cortex 16(9):1323–1331. [PubMed: 16292002]

Rees MI, Harvey K, Ward H, White JH, Evans L, Duguid IC, Hsu CC, Coleman SL, Miller J, Baer K, Waldvogel HJ, Gibbon F, Smart TG, Owen MJ, Harvey RJ, Snell RG. 2003. Isoform heterogeneity of the human gephyrin gene (GPHN), binding domains to the glycine receptor, and mutation analysis in hyperekplexia. J Biol Chem 278(27):24688–24696. [PubMed: 12684523]

Reid T, Bathoorn A, Ahmadian MR, Collard JG. 1999. Identification and characterization of hPEM-2, a guanine nucleotide exchange factor specific for Cdc42. J Biol Chem 274(47):33587–33593. [PubMed: 10559246]

Rice H, Suth S, Cavanaugh W, Bai J, Young-Pearse TL. 2010. In utero electroporation followed by primary neuronal culture for studying gene function in subset of cortical neurons. J Vis Exp(44).

Rudolph U, Mohler H. 2013. GABAA Receptor Subtypes: Therapeutic Potential in Down Syndrome, Affective Disorders, Schizophrenia, and Autism. Annu Rev Pharmacol Toxicol 54:483–507. [PubMed: 24160694]

Saiepour L, Fuchs C, Patrizi A, Sassoe-Pognetto M, Harvey RJ, Harvey K. 2010. Complex role of collybistin and gephyrin in GABAA receptor clustering. J Biol Chem 285(38):29623–29631. [PubMed: 20622020]

Schindelin J, Arganda-Carreras I, Frise E, Kaynig V, Longair M, Pietzsch T, Preibisch S, Rueden C, Saalfeld S, Schmid B, Tinevez JY, White DJ, Hartenstein V, Eliceiri K, Tomancak P, Cardona A. 2012. Fiji: an open-source platform for biological-image analysis. Nat Methods 9(7):676–682. [PubMed: 22743772]

Schneider Gasser EM, Straub CJ, Panzanelli P, Weinmann O, Sassoe-Pognetto M, Fritschy JM. 2006. Immunofluorescence in brain sections: simultaneous detection of presynaptic and postsynaptic proteins in identified neurons. Nat Protoc 1(4):1887–1897. [PubMed: 17487173]

Shimojima K, Sugawara M, Shichiji M, Mukaida S, Takayama R, Imai K, Yamamoto T. 2011. Loss-of-function mutation of collybistin is responsible for X-linked mental retardation associated with epilepsy. J Hum Genet 56(8):561–565. [PubMed: 21633362]

Soykan T, Schneeberger D, Tria G, Buechner C, Bader N, Svergun D, Tessmer I, Poulopoulos A, Papadopoulos T, Varoqueaux F, Schindelin H, Brose N. 2014. A conformational switch in collybistin determines the differentiation of inhibitory postsynapses. EMBO J 33(18):2113–2133. [PubMed: 25082542]

Tabata H, Nakajima K. 2001. Efficient in utero gene transfer system to the developing mouse brain using electroporation: visualization of neuronal migration in the developing cortex. Neuroscience 103(4):865–872. [PubMed: 11301197]

Tretter V, Mukherjee J, Maric HM, Schindelin H, Sieghart W, Moss SJ. 2012. Gephyrin, the enigmatic organizer at GABAergic synapses. Front Cell Neurosci 6:23. [PubMed: 22615685]

Tyagarajan SK, Fritschy JM. 2014. Gephyrin: a master regulator of neuronal function? Nat Rev Neurosci 15(3):141–156. [PubMed: 24552784]

Tyagarajan SK, Ghosh H, Harvey K, Fritschy JM. 2011. Collybistin splice variants differentially interact with gephyrin and Cdc42 to regulate gephyrin clustering at GABAergic synapses. J Cell Sci 124(Pt 16):2786–2796. [PubMed: 21807943]

Yu W, De Blas AL. 2008. Gephyrin expression and clustering affects the size of glutamatergic synaptic contacts. J Neurochem 104(3):830–845. [PubMed: 18199120]

Yu W, Jiang M, Miralles CP, Li RW, Chen G, de Blas AL. 2007. Gephyrin clustering is required for the stability of GABAergic synapses. Mol Cell Neurosci 36(4):484–500. [PubMed: 17916433]

Zoghbi HY. 2003. Postnatal neurodevelopmental disorders: meeting at the synapse? Science 302(5646):826–830. [PubMed: 14593168]

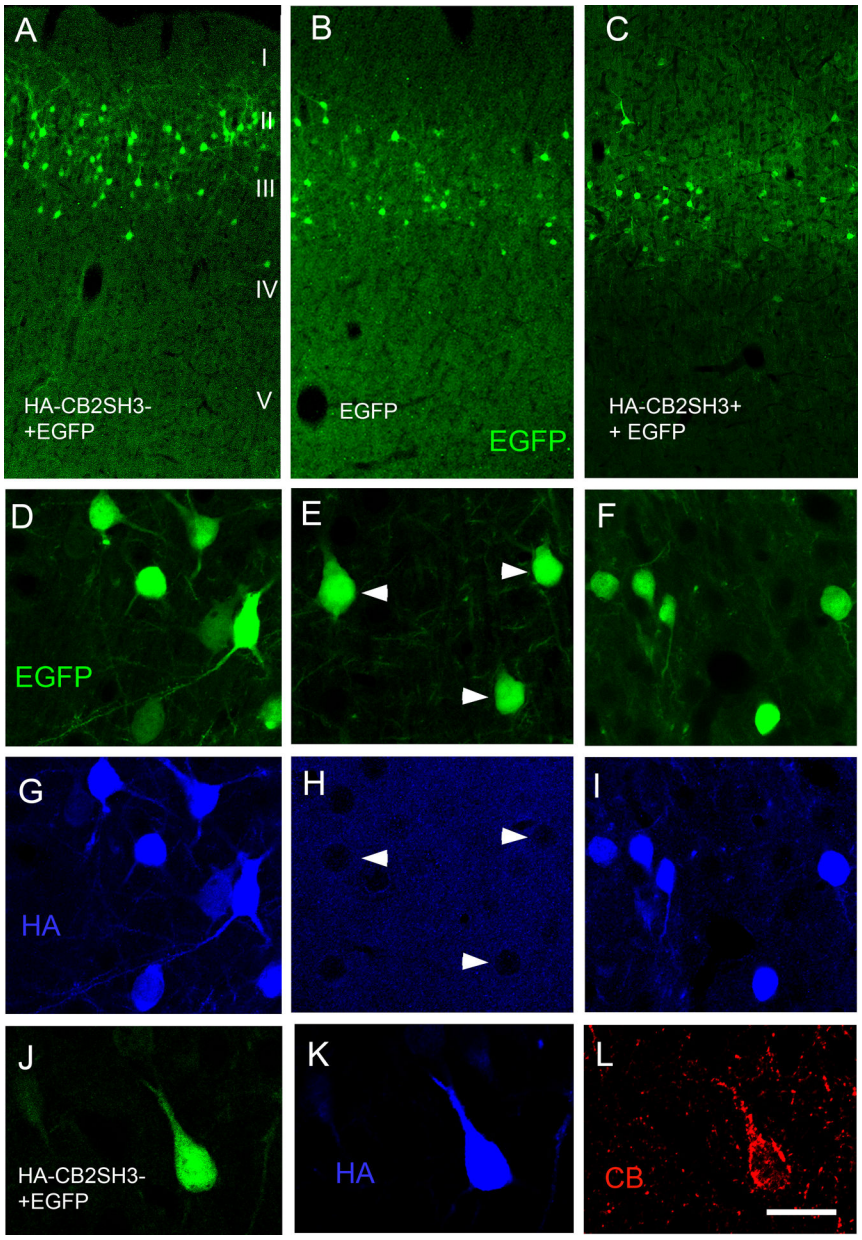

Figure 1. Cerebral cortex of rats after IUEP with $CB2_{SH3-}$ or $CB2_{SH3+}$.

Transfected neuronal precursors migrate to the appropriate cortical layer. **(A)** IUEP with $CB2_{SH3-}$ and EGFP; **(B)** IUEP with EGFP only; **(C)** IUEP with $CB2_{SH3+}$ and EGFP; **(D-I)** Double-label fluorescence of EGFP (green D-F) and anti-HA (blue G-I) of neurons transfected with $CB2_{SH3-}$ and EGFP (D and G), EGFP (E and H) and $CB2_{SH3+}$ and EGFP (F and I). Arrowheads in E and H point to neurons transfected with EGFP only, which show no anti-HA immunofluorescence. **(J-L)** Triple-label fluorescence of EGFP (green J), anti-HA (blue K) and anti-collybistin (red L) of a neuron transfected with $CB2_{SH3-}$ and EGFP. Scale bar = 250 μm in A-C; 26 μm in D-I and 17μm J-L.

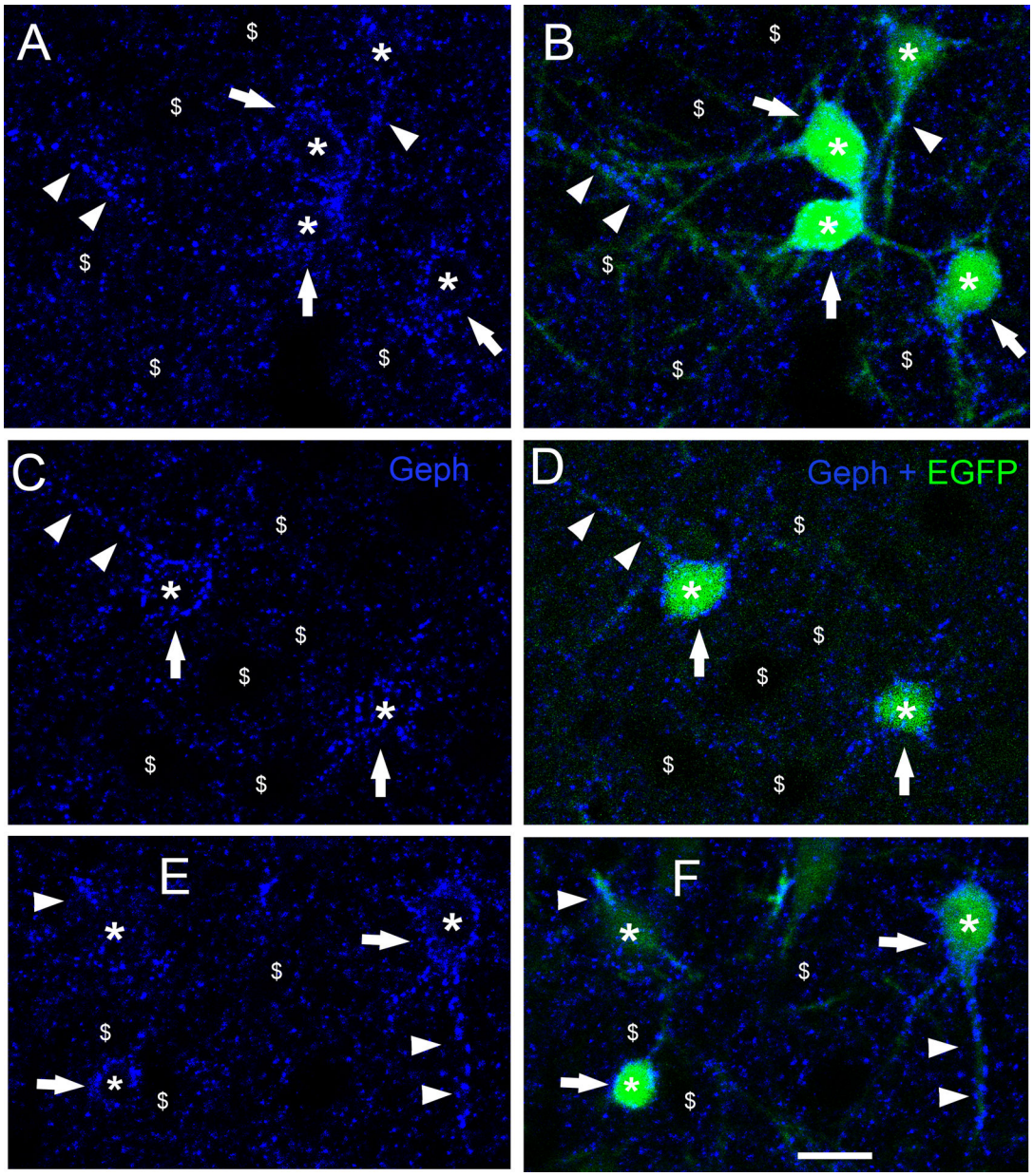

Figure 2. Neurons overexpressing CB2$_{SH3-}$ show gephyrin superclusters.

(A-F) Double fluorescence with Geph (Blue) and EGFP (green) at P45. Neurons co-transfected with CB2$_{SH3-}$ and EGFP (asterisks) have significantly larger Geph clusters (superclusters) than neighboring non-transfected neurons ($ symbol). Geph superclusters are present in somas (arrows) and dendrites (arrowheads) of the transfected neurons. B, D and F show blue and green overlays. Scale bar = 15 μm.

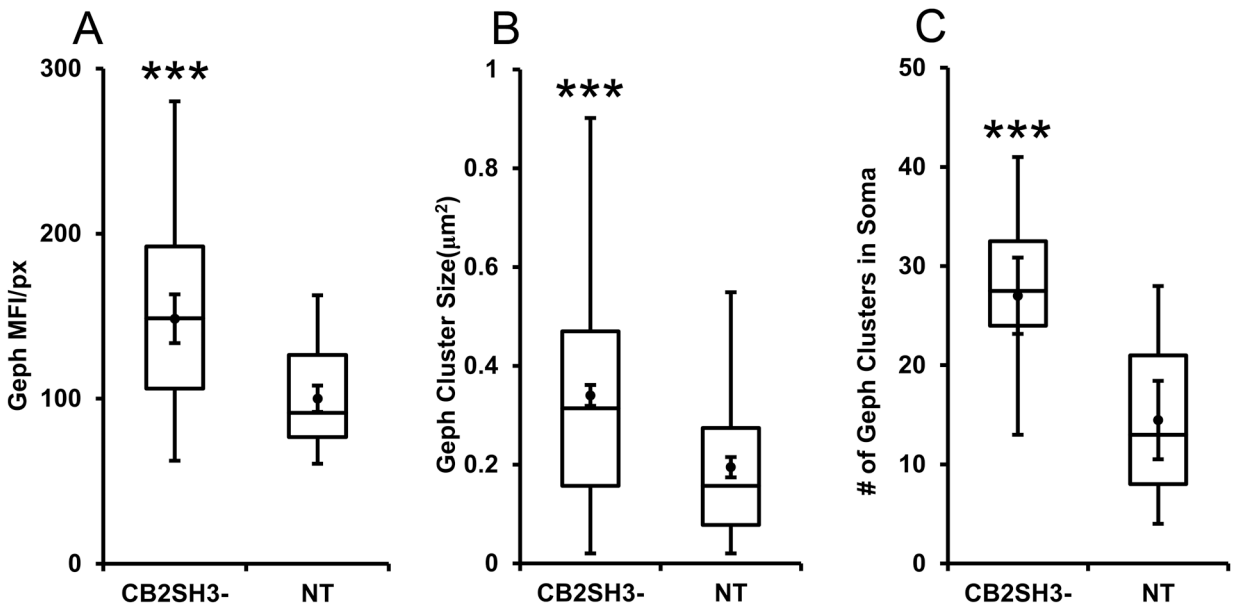

Figure 3. Quantification of the effect of $CB2_{SH3-}$ overexpression on gephyrin clusters.

The box plots display the median and interquartile range of the data while the whiskers represent the spread of the data within the 1.5 interquartile ranges of the upper and lower quartile. Inside the boxes, circles indicate mean and bars from mean indicate 95% confidence interval. **(A)** Mean fluorescence intensity per pixel of Geph immunofluorescence in $CB2_{SH3-}$ overexpressing neurons normalized to the corresponding mean value from sister non-transfected neurons at P44-P45. *** $P < 0.001$(Mann-Whitney $U=728$, $n_1=n_2=56$ neurons). **(B)** Size of Geph clusters in the somas of $CB2_{SH3-}$ overexpressing neurons compared to sister non-transfected controls*** $P < 0.001$(Mann-Whitney $U=37{,}111$ $n_1=486$ clusters, $n_2=246$ clusters). **(C)** Number of Geph clusters in the $CB2_{SH3-}$ overexpressing neurons compared to sister non-transfected controls*** $P < 0.001$(Mann-Whitney $U=38$ $n_1=18$ neurons, $n_2=17$ neurons) .

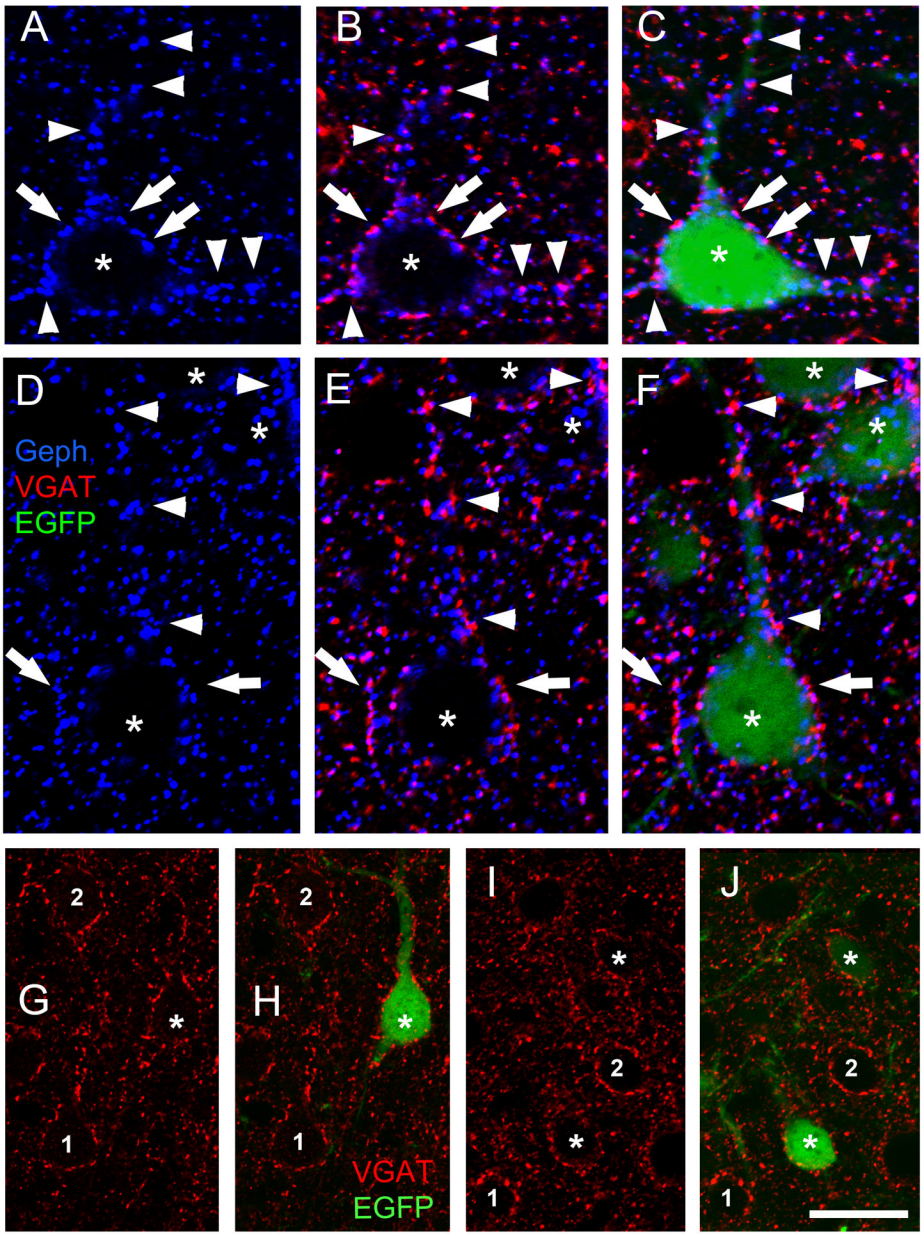

Figure 4. In CB2$_{SH3-}$ overexpressing neurons, gephyrin superclusters are associated with presynaptic vGAT puncta. However there is no effect on the extent or fluorescence intensity of the vGAT puncta contacting the transfected neuron.

(A-F) Triple-label fluorescence with anti-Geph (blue), anti-vGAT (red) and EGFP (green) at P45. Arrows and arrowheads show some examples of apposition between Geph superclusters and vGAT in somas (arrows) and dendrites (arrowheads). B and E show red and blue overlays while C and F show RGB overlays. **(G-J)** Double-label fluorescence with anti-vGAT (red) and EGFP (green). The extent and fluorescence intensity of vGAT puncta contacting CB2$_{SH3-}$ transfected neurons (green, asterisks H and J) and non-transfected neurons (numbers 1 and 2) are similar; Scale bar = 10 μm in A-F and 19 μm in G-J.

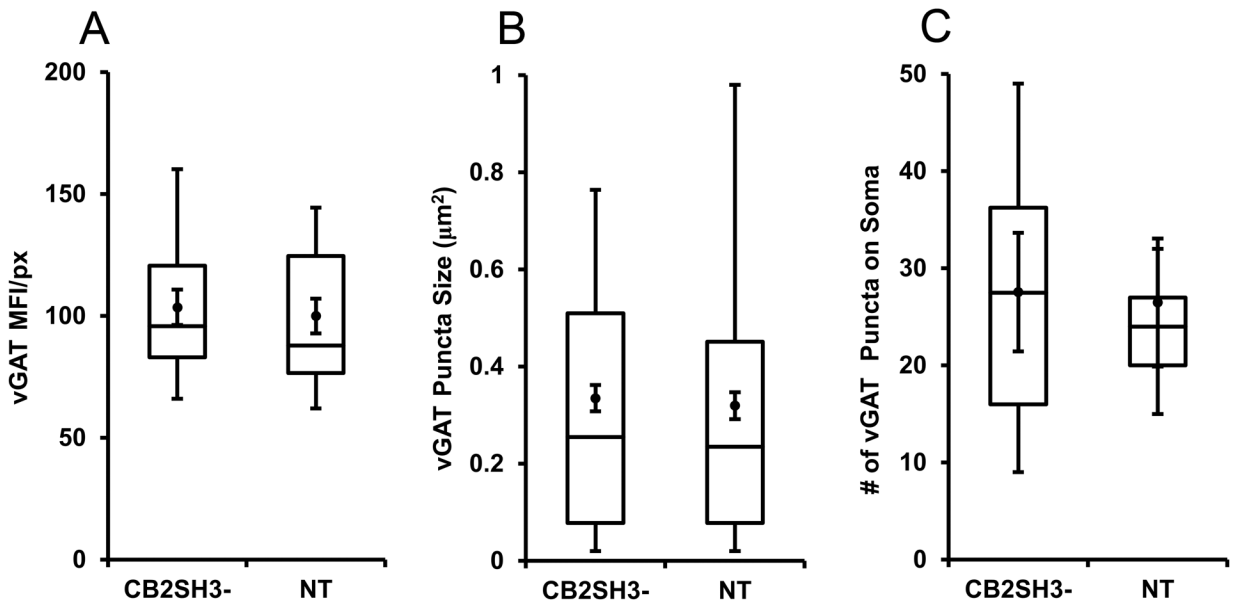

Figure 5. Quantification of the effect of $CB2_{SH3-}$ overexpression on vGAT clusters

The box plots display the median and interquartile range of the data while the whiskers represent the spread of the data within the 1.5 interquartile ranges of the upper and lower quartile. Inside the boxes, circles indicate mean and bars from mean indicate 95% confidence interval. **(A)** Mean fluorescence intensity per pixel of vGAT immunofluorescence in $CB2_{SH3-}$ overexpressing neurons normalized to the corresponding mean value from sister non-transfected neurons at P44-P45. P=0.614 (Mann-Whitney U=263, $n_1=n_2=24$ neurons). **(B)** Size of vGAT clusters in the somas of $CB2_{SH3-}$ overexpressing neurons compared to sister non-transfected controls P=0.515 (Mann-Whitney U=108,869, $n_1=496$ clusters, $n_2=450$ clusters). **(C)** Number of vGAT clusters in the $CB2_{SH3-}$ overexpressing neurons compared to sister non-transfected controls P=0.597 (Mann-Whitney U=136.5 $n_1=18$ neurons, $n_2=17$ neurons).

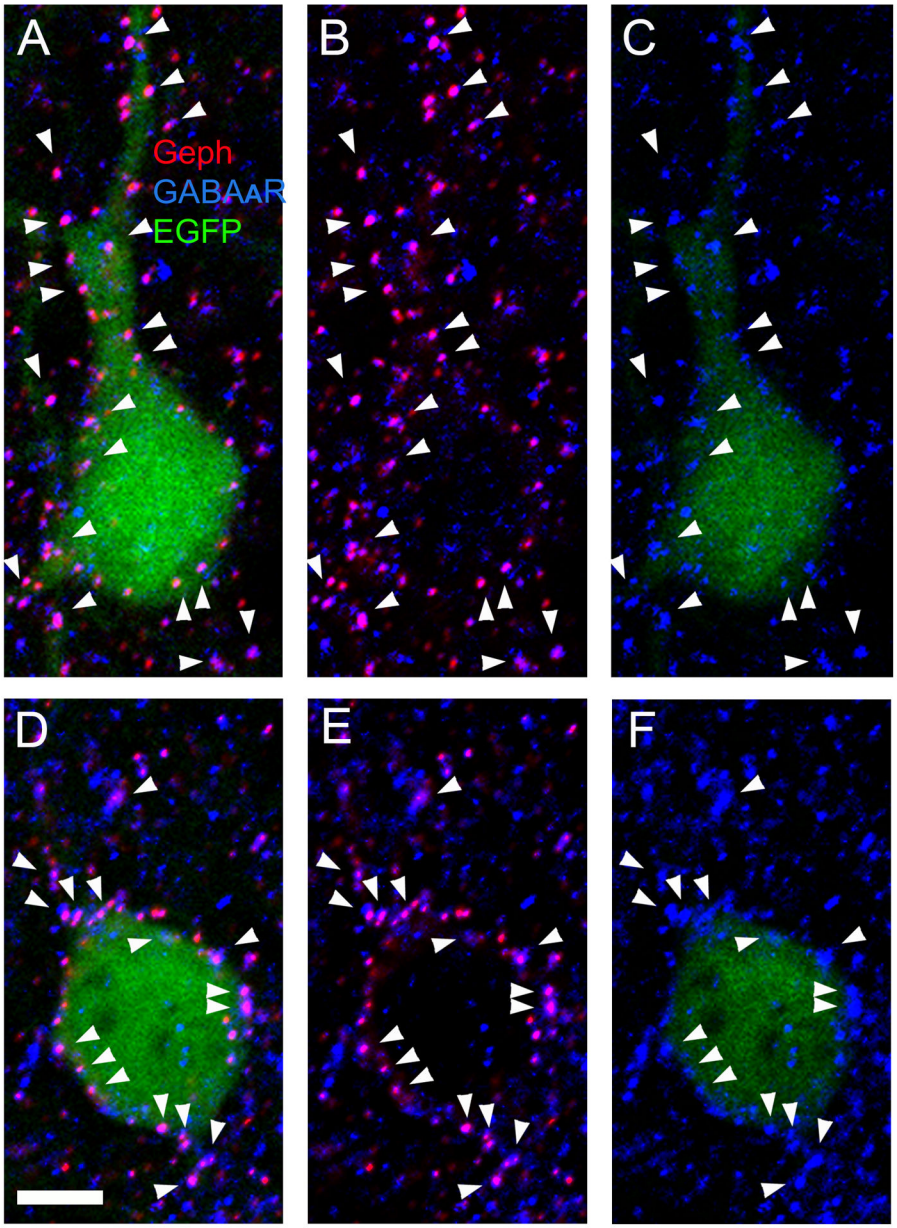

Figure 6. In CB2$_{SH3-}$ overexpressing neurons, GABA$_A$Rs co-localize with gephyrin superclusters.

(A-C and D-F) Triple-label fluorescence with anti-Geph (red), anti-γ2 GABA$_A$R subunit (blue) and EGFP (green) of two transfected cortical neurons at P45. A and D show red, green and blue overlays. B and E show red and blue overlays. C and F show green and blue overlays. Arrowheads point to co-localizing Geph and GABA$_A$R clusters. Scale bar = 5 μm.

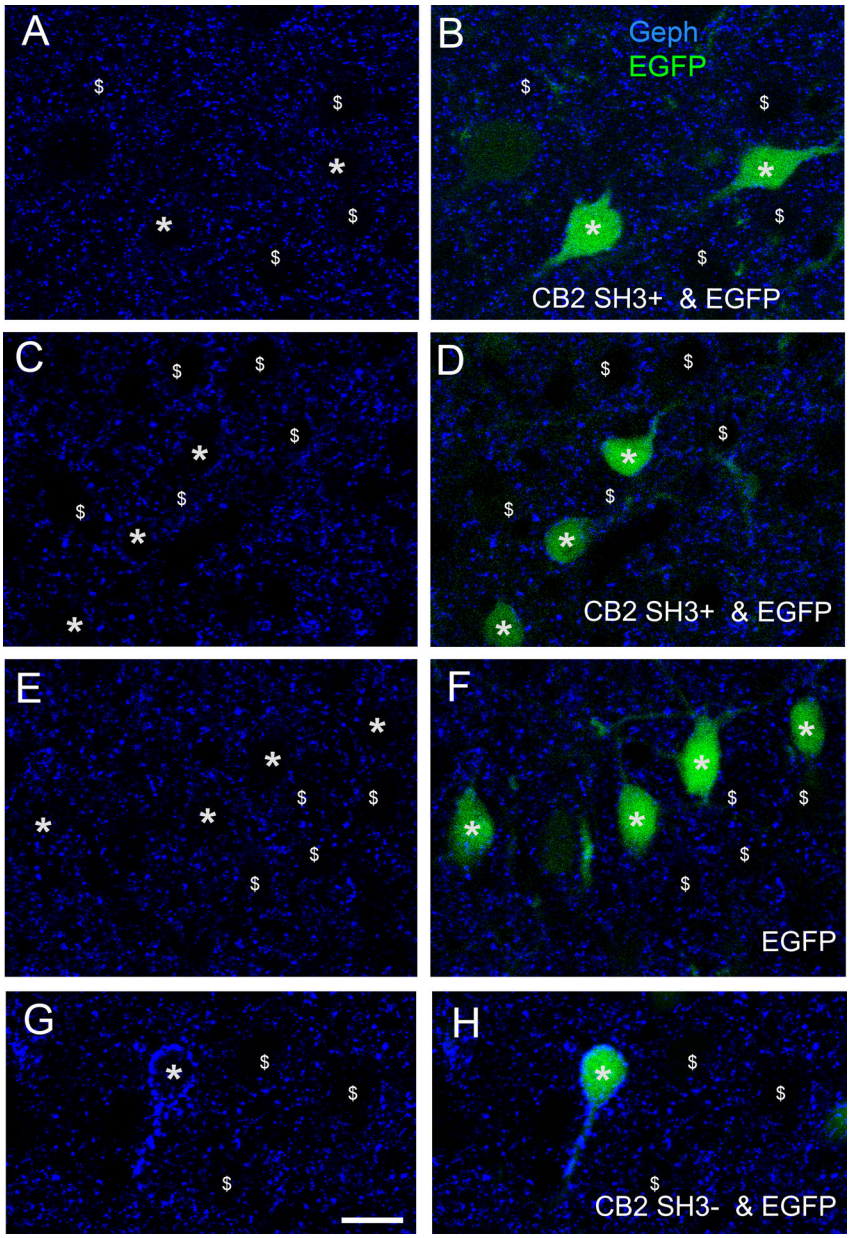

Figure 7. Neurons overexpressing CB2$_{SH3+}$ show gephyrin clusters of size similar to that of controls.

Double fluorescence with EGFP and anti-Geph at P42. **(A-D)** Neurons co-transfected with CB2$_{SH3+}$ and EGFP (green, asterisks B and D) have Geph clusters (blue) of size similar to that of neighboring non-transfected neurons ($ symbol); **(E and F)** Neurons transfected with EGFP only (green, asterisks F) have Geph clusters (blue) of size similar to that of neighboring non-transfected neurons ($ symbol); **(G and H)** For comparative purpose, neurons co-transfected with CB2$_{SH3-}$ and EGFP (green, asterisk H) have Geph clusters significantly larger than those from neurons transfected with CB2$_{SH3+}$ and EGFP (A-D) or EGFP only (E and F). B, D, F and H show the overlays. Scale bar = 15 μm.

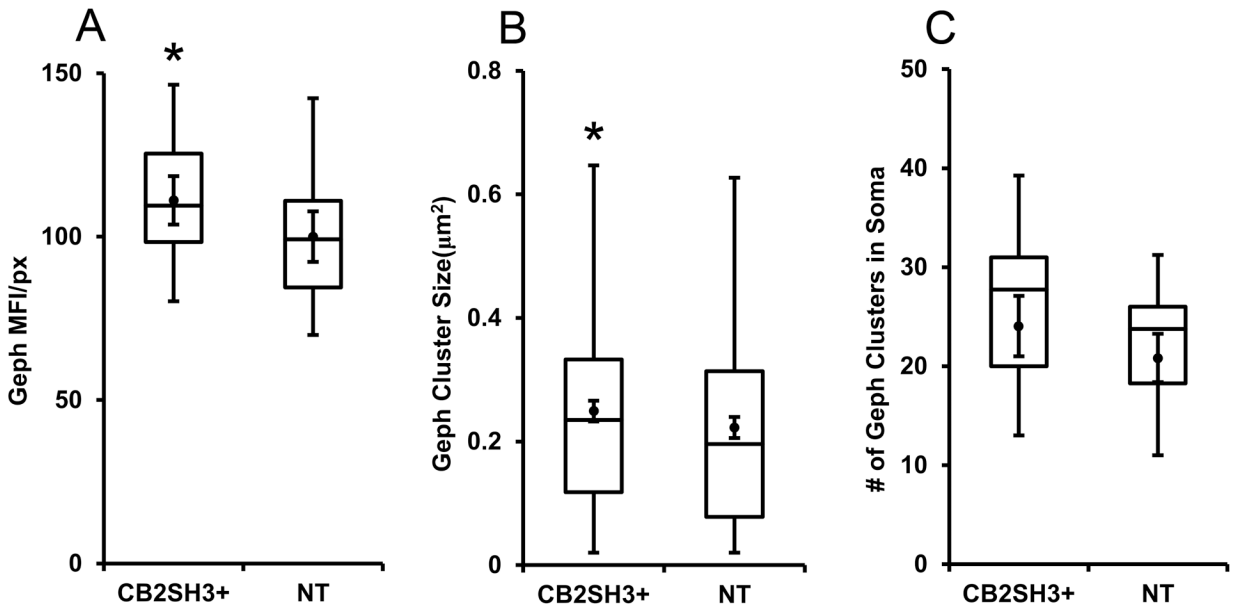

Figure 8. Quantification of the effect of $CB2_{SH3+}$ overexpression on gephyrin clusters.

The box plots display the median and interquartile range of the data while the whiskers represent the spread of the data within the 1.5 interquartile ranges of the upper and lower quartile. Inside the boxes, circles indicate mean and bars from mean indicate 95% confidence interval. **(A)** Mean fluorescence intensity per pixel of Geph immunofluorescence in $CB2_{SH3+}$ overexpressing neurons normalized to the corresponding mean value from sister non-transfected neurons at P44-P45. *P < 0.05(Mann-Whitney U=224 $n_1=n_2=26$ neurons). **(B)** Size of Geph clusters in the somas of $CB2_{SH3+}$ overexpressing neurons compared to sister non-transfected controls*P < 0.05(Mann-Whitney U=74,346 $n_1=433$ clusters, $n_2=375$ clusters). **(C)** Number of Geph clusters in the $CB2_{SH3+}$ overexpressing neurons compared to sister non-transfected controls P=0.117 (Mann-Whitney U=112 $n_1=n_2=18$ neurons) .

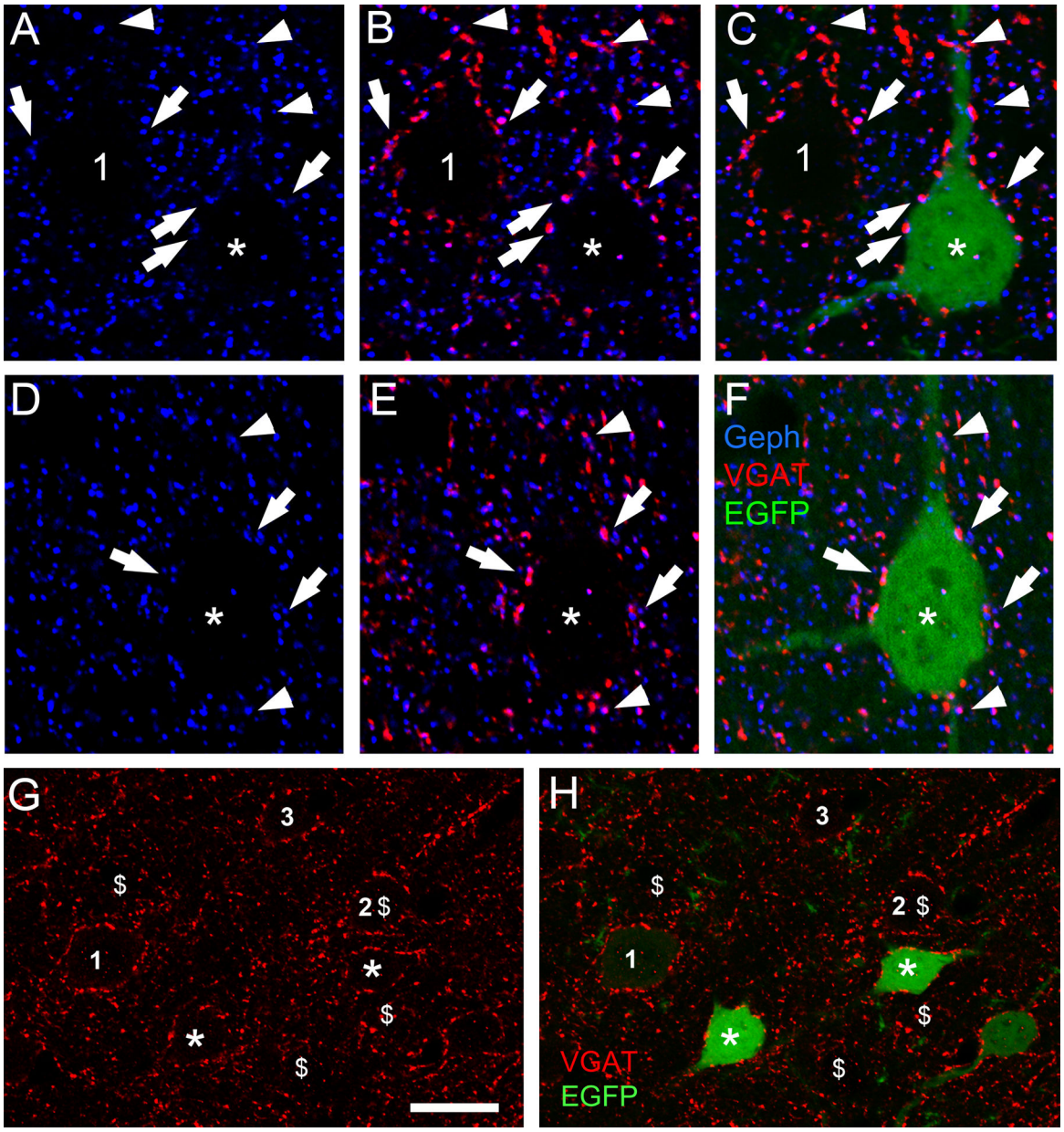

Figure 9. In CB2$_{SH3+}$ overexpressing neurons, gephyrin clusters are associated with presynaptic vGAT puncta. There is no effect on the extent or fluorescence intensity of the vGAT puncta contacting the transfected neuron.

(A-C and D-F) Triple-label fluorescence with anti-Geph (blue), anti-vGAT (red) and EGFP (green) at P42 cortical neurons. Arrows and arrowheads show some examples of apposition of Geph clusters and vGAT in somas (arrows) and dendrites (arrowheads). C and F show the RGB overlays. For comparative purposes A-C shows a transfected neuron (green, asterisk) and a non-transfected sister neuron (number 1). **(G and H)** Double-label fluorescence. The extent and fluorescence intensity of vGAT puncta (red) contacting CB2$_{SH3+}$ transfected neurons (green, asterisks) and non-transfected neurons (numbers 1–3) are similar. Note that the transfected neurons (green) in G and H are the same as in Fig 7A and B. For comparative

purposes $ symbols were added corresponding to the cells labelled with the $ symbol in Fig 7A and B. Scale bar = 10 μm in A-F and 17 μm in G and H.

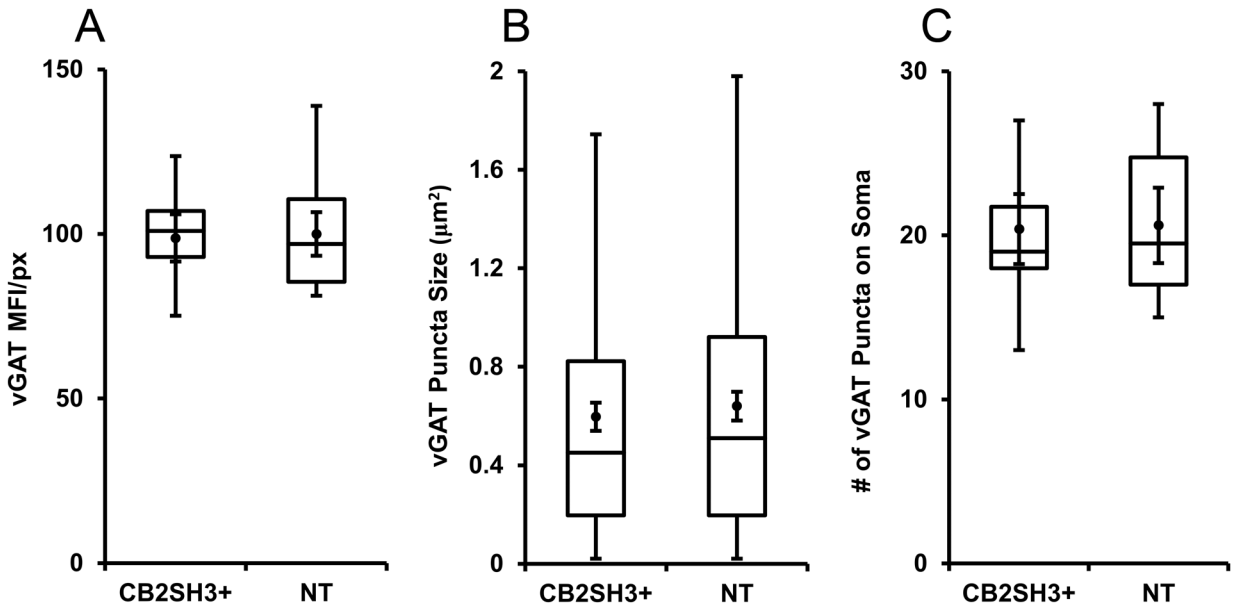

Figure 10. Quantification of the effect of $CB2_{SH3+}$ overexpression on vGAT clusters.

The box plots display the median and interquartile range of the data while the whiskers represent the spread of the data within the 1.5 interquartile ranges of the upper and lower quartile. Inside the boxes, circles indicate mean and bars from mean indicate 95% confidence interval. **(A)** Mean fluorescence intensity per pixel of vGAT immunofluorescence in $CB2_{SH3+}$ overexpressing neurons normalized to the corresponding mean value from sister non-transfected neurons at P44-P45. P=0.963 (Mann-Whitney U=336, $n_1=n_2=26$ neurons). **(B)** Size of vGAT clusters in the somas of $CB2_{SH3+}$ overexpressing neurons compared to sister non-transfected controls P=0.297 (Mann-Whitney U=65,058, , $n_1=368$ clusters, $n_2=372$ clusters). **(C)** Number of vGAT clusters in the $CB2_{SH3+}$ overexpressing neurons compared to sister non-transfected controls P=0.924 (Mann-Whitney U=158.5, $n_1=n_2=19$ neurons).

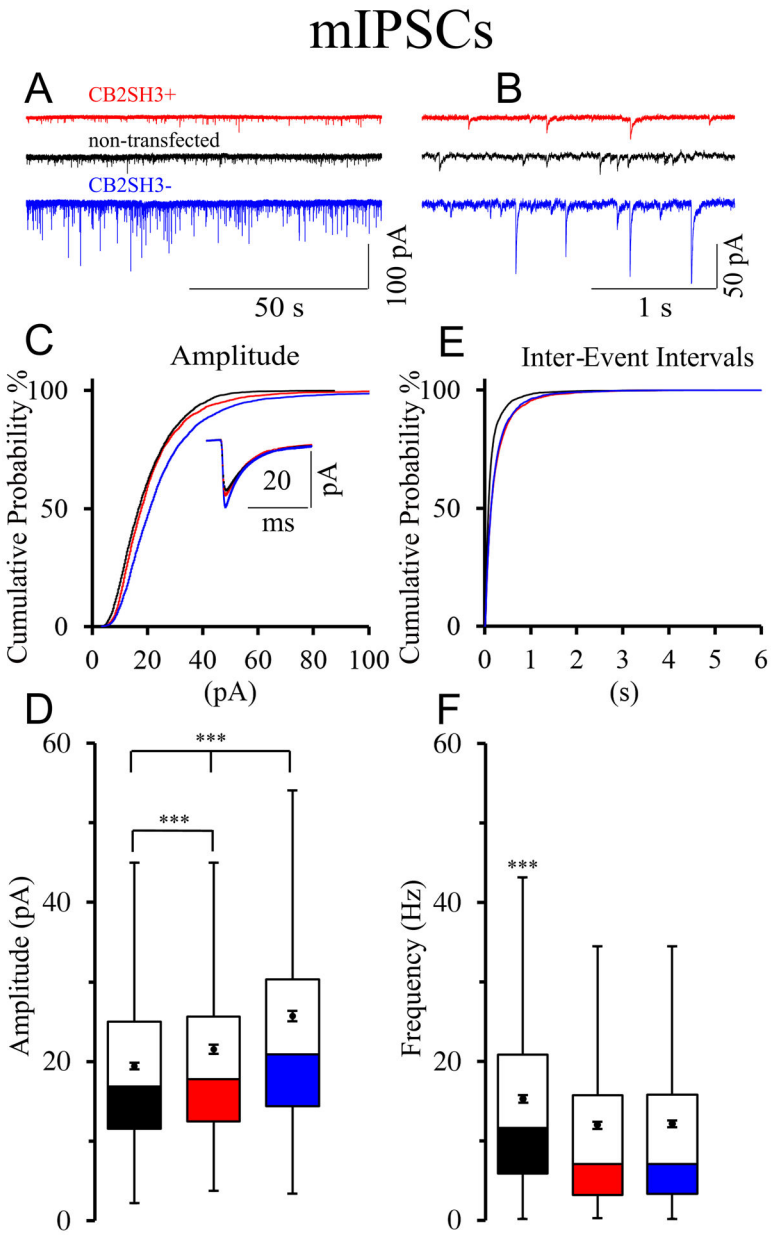

Figure 11. Overexpression of CB2$_{SH3-}$ or CB2$_{SH3+}$ increases the amplitude and decreases the frequency of mIPSCs.

(A and B) Representative traces of mIPSCs from ex-vivo recordings of neurons transfected with CB2$_{SH3-}$ (blue); CB2$_{SH3+}$ (red), and non-transfected (black). **(C)** Cumulative probability distribution of all mIPSCs amplitudes within 0–100 pA range. The mIPSCs were collected from10 CB2$_{SH3-}$ transfected neurons (n=4,197 events) from 3 IUEP animals; 9 CB2$_{SH3+}$ transfected neurons (n= 3,537 events) from 6 IUEP animals and 10 non-transfected neurons (n=3,597 events) from 5 IUEP animals. Kolmogorov-Smirnov (K-S) test indicates that the cumulative probability of the mIPSC amplitudes is significantly different ($p<0.001$) in CB2$_{SH3-}$ transfected neurons from that of either CB2$_{SH3+}$ transfected or non-transfected neurons. For the CB2$_{SH3+}$ transfected neurons, the cumulative probability of the mIPSC amplitudes was also significantly different from that of non-transfected neurons

($p<0.001$). The number of mIPSCs whose amplitudes were larger than 100 pA, not included in the graph, were 52 for $CB2_{\mathbf{SH3}-}$; 12 for $CB2_{\mathbf{SH3}+}$; and none for non-transfected neurons. The inset is an average of all mIPSCs from each condition. **(D)** Box plots of all mIPSCs amplitudes from each condition displaying median and interquartile range. Box whiskers indicate the spread of the data within 1.5 interquartile ranges of the upper and lower quartile. Inside the boxes, circles indicate mean and bars from each mean indicate 95% confidence interval. Levene's test shows unequal variance $F= 78.67$, $p<0.001$ of the samples. ANOVA Welch's test for samples with unequal variance show significant differences among the mIPSC amplitude in the three conditions ($F=142.42$ $p<0.001$). Games-Howell post-hoc test: for non-transfected to $CB2_{\mathbf{SH3}-}$ $q= 6.34$, $p<0.001$; for $CB2_{\mathbf{SH3}+}$ to $CB2_{\mathbf{SH3}-}$ $q=4.15$, $p<0.001$; for non-transfected to $CB2_{\mathbf{SH3}+}$ $q= 2.19$, $p<0.001$; **(E)** Cumulative probability distribution of the mIPSC inter-event intervals. There is a significant difference between non-transfected neurons compared to $CB2_{\mathbf{SH3}-}$ and $CB2_{\mathbf{SH3}+}$ transfected neurons (non-transfected to $CB2_{\mathbf{SH3}-}$ K-S test $p<0.001$; non-transfected to $CB2_{\mathbf{SH3}+}$ K-S test $p<0.001$; $CB2_{\mathbf{SH3}-}$ to $CB2_{\mathbf{SH3}+}$ K-S test not significant). **(F)** Box plots of instantaneous mIPSC frequency corresponding to those described in panel E. Welch's test $F=75.74$, $p<0.001$. Games-Howell test for multiple comparisons shows significant differences between non-transfected and $CB2_{\mathbf{SH3}-}$ $q=3.13$, $p<0.001$ and between non-transfected to $CB2_{\mathbf{SH3}+}$ $q=3.28$, $p<0.001$. However, the instantaneous mIPSC frequencies of neurons transfected with either $CB2_{\mathbf{SH3}-}$ or $CB2_{\mathbf{SH3}+}$ were not significantly different ($q=0.15$, $p=0.876$). The GABAergic nature of the mIPSCs was confirmed by their blockage with 10 μM of gabazine ($GABA_A$ receptor antagonist, data not shown).

TABLE 1

Primary Antibodies Used

Antigen	Immunogen	Manufacturer, catalog #, lot#, RRID, species, mono/polyclonal	Dilution
Collybistin	Recombinant protein (aa 4–229 of rat collybistin).	Synaptic systems; 261 003; lot# 261003/3; Rabbit; Polyclonal	1:500
γ2 subunit of the GABAA Receptor	synthetic peptide QKSDDDYEDYASNKT	RRID: AB_2314477; Rabbit; Polyclonal	1:10
Gephyrin	Purified Glycine receptor/gephyrin complex from rat spinal cord	Synaptic Systems; 147021; lot#147021/9; RRID:AB_1279448; Mouse; Monoclonal	1:200
HA	synthetic peptide CYPYDVPDYASL	Covance; MMS-101R; Clone 16B12; lot# E11EF01029; RRID:AB_10064220; Mouse; Monoclonal	1:500
vGAT	Strep-Tag fusion protein of rat vGAT (aa 2 – 115)	Synaptic Systems; 131004; lot#131004/13; RRID:AB_887873; Guinea Pig; Polyclonal	1:1,000